Title

THE TECHNOLOGY AND USES OF LIQUID HYDROGEN: LIQUID HYDROGEN BUBBLE CHAMBERS

Authors

Hernandez, H. Paul
Birmingham, Bascom W.

Publication Date

1962-07-11

University of California

Ernest O. Lawrence Radiation Laboratory

Berkeley, California

DISCLAIMER

UCRL-10358

For Chapter in book

UNIVERSITY OF CALIFORNIA

Lawrence Radiation Laboratory
Berkeley, California

Contract No. W-7405-eng-48

THE TECHNOLOGY AND USES OF LIQUID HYDROGEN: LIQUID HYDROGEN BUBBLE CHAMBERS

H. Paul Hernandez and Bascom W. Birmingham

July 11, 1962

THE TECHNOLOGY AND USES OF LIQUID HYDROGEN

CHAPTER 9

Liquid Hydrogen Bubble Chambers

H. Paul Hernandez* and Bascom W. Birmingham†

*Lawrence Radiation Laboratory, Berkeley, California.

†Cryogenic Engineering Laboratory, National Bureau of Standards, Boulder, Colorado.

SECTION I

INTRODUCTION

INTRODUCTION
PHYSICS EXPERIMENT
HISTORY AND EVOLUTION

INTRODUCTION

Progress in high-energy nuclear physics over the past 25 years has been made possible largely by improvements in accelerator design and in the art of particle detection.[1] One of the newest and most powerful detectors now used to observe these particle interactions is the liquid hydrogen bubble chamber.

An accelerator yields a large number of particles per pulse. Further advantages are that particles of a particular kind can be selected, they all come from the same direction, and energy limits can be set. High-energy particles occur naturally in our atmosphere as cosmic rays, but they come from many directions and are made up of particles of different kinds and of many energies. Before accelerators existed, nature was the only source of high-energy particles, but the yield of cosmic-ray experiments was very low and perhaps might be compared to the difference between the speed of hand computation and modern computers.

Today a major part of high-energy physics is concerned with "strange particles" such as K mesons and hyperons. Strange particles were first observed in 1947 at the University of Manchester in England. They were found quite by accident and had a strange property: a lifetime of 10^{-10} second, or 10^{11} times longer than existing theory predicted.[2]

By 1959 ten strange particles had been discovered, and such things as their mass, charge, lifetime, and some details of their decay were known. Today about thirty different kinds of strange particles have been observed, but a general theory does not yet exist to account for their behavior as the quantum theory explains the periodic table. The strange-particle problem is very similar to the riddle of the elements that faced early scientists before the periodic table was established.

A bubble chamber is a closed vessel filled with a transparent liquid. A 4-inch bubble chamber is shown in Fig. 1 and the parts identified on Fig. 8. The operation of a bubble chamber can be visualized by means of a P-V-T diagram as shown in Fig. 2. The liquid in the chamber is held subcooled at a temperature above the normal boiling point and at a pressure high enough to prevent boiling,[3,4] as indicated by point (1). When the pressure on the liquid is suddenly lowered by adiabatically expanding the liquid along the path (1) (2) (3) to a point below the saturated vapor pressure and in the superheated range (point (3)), the liquid becomes thermodynamically unstable. The unstable superheated liquid will evaporate until an equilibrium pressure is reached again. In a bubble chamber the degree of superheat is controlled so that the bubbles are nucleated by ionized particles before spontaneous boiling occurs. When a charged particle passes through the chamber liquid, it ionizes atoms of the chamber fluid along its path. A series of bubble nuclei is formed owing to the sudden increase in the local thermal-energy density.[5,6] The particle, which passes through the chamber in microseconds, leaves a trail—made up of a string of bubbles—that persists long enough to be photographed (Fig. 3).

The pressure cycle of a bubble chamber starts with an expansion that must be rapid enough to reach the unstable point (3). While the chamber is at the low expanded pressure (3), the particle passes through the chamber, and the chamber is recompressed quickly to its initial condition (1) where it waits for the next pulse. A complete pulse typically takes about 25 msec and is repeated every few seconds. When the chamber liquid is expanded and compressed quickly, it compresses essentially along the same path as that along which it expanded i.e., (3) (2) (1); the net P-V work is essentially zero. If the expansion were slow enough the fluid would expand adiabatically from

① to ② and then isobarically along the equilibrium line ② to ④ and the chamber would not form tracks.

PHYSICS EXPERIMENT

The particle event observed in the bubble chamber is photographed in three-dimensions, giving a permanent record for later study. One such system is shown in Fig. 4. The high-energy particles leaving an accelerator are often protons. These protons, with energies as high as 30 BeV, the limit of today's accelerators, strike a target which may be simply a small piece of copper. The protons enter the copper atoms and strike the nuclei, giving off a great shower of particles of many kinds and of many energies and traveling in almost all directions. A small solid angle of secondary particles is collimated and passed through bending magnets which select particles to given momentum limits (Fig. 5). These particles may be further screened by high-voltage spectrometers that select particles within certain velocity ranges. In addition, focusing magnets located along the path focus the beam of selected particles into a small pencil to confine the beam within the beam pipe and to increase the particle density. The particles leaving the completed beam path give a beam that is made up of only one kind of particle, say negative protons (antiprotons), having specific energy limits and having a given number of particles per pulse.

This beam of selected particles continues on through the metal walls of the bubble chamber (metal is mostly space relative to the size of the particle) and finally through the bubble-chamber liquid. As particles pass through the liquid they may strike the nucleus of an atom of the liquid; and if other charged particles are knocked from the nucleus, they will form additional tracks or stars (Fig. 6). It is these tracks, made up of fragments from the collision with the nucleus, that are studied. By looking at a sufficient

number, statistical conclusions can be made. Uncharged particles do not nucleate bubbles, and so they do not leave visible trails.

The charge of the particle making the track is determined by a magnetic field that passes through the chamber normal to the tracks. The field curves the flight of the particles through the chamber, leaving a track that is curved clockwise or counter-clockwise, depending upon whether the charge of the particle is positive or negative. The density and size of the bubbles identify the mass of the particle and the mass together with the radius of curvature of the tracks establish the momentum.

HISTORY AND EVOLUTION

It might be worthwile to ask why the bubble chamber was not invented until 1953. Every bit of the theory and all of the experimental techniques were available fifty years ago when the cloud chamber was developed. The reason is largely that there was no incentive to go toward higher densities in cloud-chamber-like devices. Lawrence did not invent the cyclotron until a quarter of a century after Wilson invented the cloud chamber. Cloud chambers were the predecessors of bubble chambers and operate very similarly, but rather than being filled with liquid they are filled with saturated water vapor (Fig. 2). The cloud chamber is suddenly expanded adiabatically (from point (5) to (6)) so that the air contains more water vapor than necessary for saturation. Molecules of the air-water mixture are ionized by the beam passing through the chamber, and act as condensation nuclei. The excess water vapor separates out on these ions and will form a string of fine droplets of liquid, which appears as a track suspended in the cloud chamber.[7]

As Professor Luis W. Alvarez pointed out, "The bubble chamber is one of the best examples of an essential invention in the detection field, which

came about in answer to a very great need. Donald Glaser was aware of the shortcomings of the cloud chamber for high energy experiments, and set about in a systematic way to invent a device which would incorporate its good features, and eliminate its drawbacks. The most obvious disadvantage of the cloud chamber is the low density of its gas — the number of nuclear events per unit length of particle track is of course directly proportional to the density of the material."

The density of bubble-chamber liquid is from 700 to 1000 times as large as the density of gas used in cloud chambers. Cloud chambers have long recovery times and can only be operated about once every two minutes, whereas bubble chambers have operated as fast as 20 pulses per second.[8] The number of nuclear events per unit time recorded in a bubble chamber is about 50 000 times the quantity recorded in a cloud chamber.

Donald L. Glaser was awarded a Nobel Prize for his invention of the bubble chamber, which he invented in May 1952 while at the University of Michigan in Ann Arbor. His first bubble chamber was made of a glass tube about 4 inches long and 0.01-inch inside diameter filled with diethyl ether[9,10] (Fig. 7).

The value of this new detector was recognized early by Professor Luis W. Alvarez of the Lawrence Radiation Laboratory (LRL) at Berkeley, and by 1954 his group had a 4-inch-diameter chamber in operation. It was filled with 0.4 liter of liquid hydrogen.[11,12] (Figs. 1 and 8).

By May 1956 a 10-inch-diameter bubble chamber holding 9 liters of liquid hydrogen (Fig. 9) was operating with the Bevatron in Berkeley, and by late 1957 the 15-inch bubble chamber was in operation.[13,14]

Within the next year many bubble chambers were in operation at laboratories all over the world. Some operated with liquid hydrogen and deuterium but others used propane, argon, or helium for working fluid, and one built by Glaser used liquid xenon.[15]

In early 1955, when the world's largest bubble chamber was only 4 inches in diameter, the decision was made by Alvarez to build a 72-inch-long bubble chamber holding over 500 liters of liquid hydrogen (Fig. 10). Tracks were observed on its first operation in March 1959, four years after its conception. The 72-inch bubble chamber has been in operation since that time, mostly with liquid hydrogen but it has also operated for over a month with 500 liters of liquid deuterium. The chamber has been kept filled with liquid hydrogen for as long as ten months.

At present there are three other large liquid hydrogen bubble chambers under construction. The 60-inch British National bubble chamber, which is scheduled to be completed at the end of 1962, is shown on Fig. 11.[16,17] The British National bubble chamber has been designed and constructed in England, and will be transported to the CERN Laboratory in Geneva where it will first operate with the 27-BeV AGS proton-synchrotron.

A 2-meter bubble chamber, which will hold 1080 liters of liquid hydrogen and will weight over 600 tons, is now under construction by the CERN Laboratory and is estimated to be completed by the end of 1963.[18] At the Brookhaven National Laboratory, New York, an 80-inch chamber with a capacity of 1470 liters of liquid hydrogen is scheduled to be operating in 1963.[19]

SECTION II

LIQUID HYDROGEN BUBBLE CHAMBER DESIGN PARAMETERS

LIQUID HYDROGEN BUBBLE CHAMBERS
BUBBLE CHAMBER OPERATING CONDITIONS
CONTAMINANTS

LIQUID HYDROGEN BUBBLE CHAMBERS

The choice of a liquid in a bubble chamber is governed largely by the kind of information desired from the high-energy events to be studied. For elementary particle production processes or their secondary reactions, hydrogen, deuterium or helium are the most desirable.[20]

A bubble chamber filled with liquid hydrogen constitutes a target of pure protons and together with a beam of particles of a single kind and energy is a great convenience to the physicist. He does not have to tediously separate out unwanted events but can concentrate directly on the elementary productions and interactions.

The dimensions and shape of the bubble chamber are determined by the kinds of experiments to be performed. The total expenditure of funds is determined when the minimum error in the measurement is specified. Some optimization can then be made between the chamber dimensions and the magnetic field strength. The chamber, to be useful in high-energy physics, should have not less than 10 liters of visible liquid hydrogen. So far there appears to be no upper limit in size. At present it seems likely that the next generation of big chambers will not increase very much in cross section over present chambers, which are about 30 inches wide by 20 inches deep, but may be twice as long, perhaps 12 to 15 feet.

The chamber pulse rate or expansion rate is usually matched to the number of pulses per minute that the accelerator will furnish. Pulse rates have been about one pulse every six seconds, but the new accelerators are faster and pulse rates are as fast as one pulse every 50 msec. Other considerations in selecting the pulse rate are that the refrigeration system must be able to keep up with the inefficiencies of expansion and recompression of the chamber fluid. The time between pulses must be long enough to compress

out the bubbles and to permit the chamber fluid to reach a quiet state. The chamber design also must be such that the fluid velocities during the expansion are not so high as to cause distortion of the tracks. That is, the photograph must be taken before the bubble is moved from the location where it is nucleated.

BUBBLE CHAMBER OPERATING CONDITIONS

The liquid hydrogen operating temperature has been different for almost every bubble chamber, but it has always fallen between the limits of 25 to 29°K because of the bubble growth characteristics and the similarity of bubble chamber geometry. The operating temperatures and pressures of several bubble chambers are shown in Fig. 12.

A small fast "clean" chamber will operate at a lower temperature than a large slow "dirty" chamber. It is easier to design a small chamber to expand rapidly than it is a large chamber, simply because it is easier to move small masses quickly; but in principle, size alone does not determine the speed or the temperature.

When bubble chambers reached diameters of 2 to 4 inches, they were then made with glass windows bolted to metal bodies. Bubble chambers of this design were called "dirty" when compared to the early all-glass "clean" chambers. The added irregularities and sharp corners of the glass-and-metal chambers nucleated many more bubbles than the smooth all-glass types. These irregularities caused the threshold pressure for spontaneous boiling to increase. This made it difficult to expand the chamber to a low pressure, because the chamber must expand faster than gas is formed by local boiling of the liquid. The bubble chamber operating cycle will be described by the pressure-temperature diagram (Fig. 12) and the pressure-pulse diagram (Fig. 13).

The words "fast" and "slow" relate to the time required to expand the liquid hydrogen in the chamber from the initial pressure to the expanded pressure (Fig. 13). A fast expansion time is very important because during the expansion cycle the fluid becomes thermodynamically unstable as soon as the saturation line is crossed. The instability of the liquid is a function of the fluid temperature, the time required to expand the chamber, and how far the pressure is below the vapor-pressure line. A fast expansion time is desirable because less time is spent in the unstable region before the particle beam enters the chamber and the picture is taken. Fast expansion also allows lower pressures to be reached, a broader pressure-temperature operating zone, and less spontaneous boiling. In early bubble chambers the expansion times were often limited by the impedance of the expansion line connecting the chamber to the expansion system. That is, the expansion line was a restriction between the chamber and the expansion system.

The second part of the expansion cycle (Fig. 13), usually called the "bottom of the valley," has a width that is determined by the rate of bubble growth, how accurately the accelerator beam can be controlled and repeated in time (jitter), and the length of the bubble chamber. The bubble growth rates at all temperatures are fast relative to the chamber valley widths, but still the amount of dwell-time waiting for bubbles to grow is the primary factor. Particle accelerators now can control their particle beams so that the beam appears at the same place on every expansion cycle within a few hundred microseconds. Long bubble chambers may need a wider valley because time must be allowed for the chamber to become sensitive over its entire length. For example, on the 72-inch bubble chamber the expansion cycle at one end of the chamber leads the far end by about 3 msec, because the sonic velocity through the hydrogen determines the rate at which the pressure

wave travels through the chamber. However, if the chamber can be made to expand in a different mode so that the expansion is only across the width or narrow dimension, then the length of the bubble chamber would not effect the valley width.

The recompression time is also important. A fast recompression time reduces the amount of boiling, lowers the convection currents, and thus reduces the temperature gradients.

A small temperature gradient is important for three reasons. The principal reason is that a constant fluid temperature gives tracks of uniform density. The second reason is that a uniform temperature will give a uniform index of refraction, which is necessary to avoid optical distortion, especially when photographing through deep chambers. The third reason is that the initial pressure before expansion is determined by the hottest spot in the chamber. That is, the initial pressure may be about 5 lb over the vapor pressure corresponding to the chamber bulk temperature. This is so because there is fluid somewhere in the chamber above the bulk temperature and at a vapor pressure corresponding to the overpressure. The overpressure prevents the fluid in the chamber from evaporating slowly between pulses. The overpressure is wasted load on the refrigerator, because it increases the energy per pulse by requiring a larger pressure ratio. With a fixed expansion ratio the use of overpressure prevents the chamber from expanding to as low a pressure and hence may limit the operating range of the chamber.

The operating range of temperature and pressure can be selected after the fluids to be used in the chamber have been determined. The first cryogenic chambers were designed for only one fluid, such as hydrogen or helium. Now chambers are designed to operate with either hydrogen, deuterium, or helium.

When the fluids have been selected, the operating temperatures can be empirically chosen from experimental data of previous chambers. For liquid hydrogen 27°K is a common design temperature. The width of the temperature band, say from 25 to 29°K, for hydrogen is only a refrigerator control problem, but whether or not the chamber is "sensitive" throughout the temperature range depends upon the ability of the chamber to reach a low expanded pressure. When the chamber is operating, the expanded pressure is adjusted by changing the bubble chamber expansion ratio until good tracks are obtained. The sensitivity of the chamber could also be changed by varying the operating temperature, but this would be very slow because a new temperature equilibrium has to be reached.

The expansion system is designed to produce expansion ratios and expansion speeds over a range that has been known to work before. The absolute value of the expanded pressures reported to form good tracks are scattered within one-third of an atmosphere. Whether this is a variation due to the chamber characteristics or due to pressure-measuring errors is not known. The pressure - time information is displayed on an oscilloscope and is used to monitor the chamber performance, rather than to obtain absolute pressure values.

The expansion system permits a change in volume of the chamber and must allow the chamber to expand an amount equal to the compressibility of the liquid for the given pressure ratio and the volume of the gas formed by local boiling:

$$\Delta V_{exp} = \Delta V_{liq} + \Delta V_{gas} .$$

The compression properties of the hydrogen can be predicted much more accurately than the volume of gas that will be formed from spontaneous boiling or flashing. The amount of volume change in the expansion system to

allow for the compressibility of the chamber liquid can be estimated with errors no greater in magnitude than other assumptions that must be made. The operating experience of many bubble chambers was shown in Fig. 12, which gives the approximate expanded pressure required to obtain good tracks at various temperatures. An average expansion pressure line derived from values on Fig. 12 is drawn in the superheated zone of the P-V diagram in Fig. 14. For any operating temperature the change in volume of the liquid as the pressure is reduced from the saturated pressure to the expanded pressure can be obtained if we can made some prediction about the liquid hydrogen expansion process.

Isothermal lines are known in the subcooled region[21] and have been extrapolated below the saturation line by superimposing a curve of the van der Waals form on the known P-V data.[22] Isentropic curves were then calculated for the superheated range, starting from the intersection of the isothermal line and the saturation line.

The isothermal line does not necessarily represent an upper limit but rather a reference line. An isentropic expansion is, however, the limiting "best" case for a bubble chamber expansion.

The P-V data from Fig. 14 are again shown as $\Delta V/V$ versus T on Fig. 15, which shows some operating points for bubble chambers having a liquid expansion system, such as a piston or bellows. The $\Delta V/V$ of these chambers is the amount of volume change in the expansion system, obtained by measuring the piston displacement. The most efficient bubble chambers operate close to the isentropic line. High efficiency means that the expansion volume of the gas formed by boiling is very small, because the piston or bellows is cold enough and fast enough to prevent local boiling, and the coupling of the piston to the chamber is very good.

CONTAMINANTS

The bubble chamber can be contaminated—so that tracks cannot be seen—by either contaminants in the chamber fluid itself or by the condensing of gases on optical surfaces.

When operating with liquid deuterium, the tritium content must be less than 1 part in 10^{13}. Tritium is an unstable hydrogen isotope and emits beta particles (fast electrons). The beta particles nucleate the deuterium and create spurious background tracks, so that the chamber has a milk-like appearance.

Helium gas is slightly soluble in liquid hydrogen and can also contaminate a bubble chamber.[23] Helium gas is used to pressurize inflatable gaskets that are used to seal the glass window to the chamber. If gas enters the chamber from leaks in the inflatable-gasket system, the gas will dissolve in the liquid hydrogen and increase the $\Delta V/V$ of the liquid. It will then be more difficult for the expansion system to expand the chamber to a low enough pressure to make tracks.

Another form of helium contamination is caused when particles from the accelerator beam strike a helium molecule and make unwanted tracks in the chamber. These tracks make film analysis more difficult.

Mechanical contaminants such as water, air, carbon dioxide, oxygen, nitrogen, and other gases that solidify above the operating temperature of the chamber may condense on the glass or other optical surfaces so that the tracks are not visible through the fogged glass or the light is badly reflected. These contaminants can be either inside or outside the chamber. The layer condensed on the glass need only be thick enough to cause a quarter-wave shift in the light path. This requires that contaminants in the chamber liquid be less than 1 part in 10^{7}.

SECTION III

DESIGN AND CONSTRUCTION OF LARGE BUBBLE CHAMBERS

CHAMBER ORIENTATION AND ARRANGEMENT
CHAMBER ASSEMBLY
CHAMBER BODY
CHAMBER WINDOW
INFLATABLE GASKET
    Chamber Prestress
VACUUM SYSTEM
NITROGEN SHIELD
EXPANSION SYSTEM
MAGNET
    Magnet Walking System
    Photographic System
TRACKS AND BUBBLE SIZE

CHAMBER ORIENTATION AND ARRANGEMENT

Chambers have been made with one or two windows and are oriented with the windows vertical or horizontal. Operational difficulties, such as keeping spurious bubbles out of the visible region in the chamber, are easily solved for either vertical or horizontal window designs. Window fogging is an operational accident and has happened on both types.

There have been two general arrangements used. One arrangement requires that the magnet, which weighs about 500 tons, and the vacuum tank be made in two pieces which are brought together on a transport system and assembled around the chamber. This arrangement is used in the 80-inch Brookhaven chamber (Fig. 16), the CERN 2-meter chamber, and the 60-inch British National chamber (Fig.17A).

Another arrangement, used on the Lawrence Radiation Laboratory's 72-inch bubble chamber, suspends the chamber from a top plate (Fig. 18). Chambers with this arrangement are easily assembled by lowering them into the vacuum tank, which normally stays in the magnet. The description in this section will be based on the Berkeley 72-inch bubble chamber. Also, the differences from the other large chambers will be noted.

After considerable study of the possible ways of bringing particle beams into the chamber and of the mechanical assembly problems, a horizontal window design was adopted for the 72-inch bubble chamber.[24] This choice, as opposed to a design having one or more vertical viewing surfaces, does bring in some problems relating to the thermal gradients in the liquid. However, it was felt that the research advantages far outweighed the difficulties involved, and experience appears to bear out this conclusion.

A one-window viewing system is employed, which permits the use of a pole piece in the magnet, giving substantially more magnetic field than would

otherwise have been available. The one-window system also contributes to operational safety since the chamber, hydrogen shield, and top plate form a closed region isolated from the main insulating vacuum region—in the event of window failure. (Fig. 19).

Figure 20, a cutaway model, reveals the main components of the 72-inch bubble chamber. The chamber body, which contains 520 liters of liquid hydrogen, can be seen suspended inside a vacuum tank. This tank is placed inside a large electromagnet. The camera and light source are mounted on the cover plate of the vacuum tank.

CHAMBER ASSEMBLY

Figure 18 shows the 72-inch bubble chamber and its related parts in greater detail. The incoming beam of high-energy particles enters the liquid via two thin stainless steel "windows", one in the vacuum tank and one in the chamber body. Because these windows are only 0.039-inch thick, the beam can pass through with a negligible amount of scattering.

CHAMBER BODY

The shape of all large bubble chambers designed up to this time has been oblong with one or two glass windows that extend the full length of the chamber. The oblong shape fits the experimental geometry and conserves the liquid hydrogen volume. The glass window on an oblong chamber may be narrower and thinner than on a circular chamber. However, an oblong shape with one or two glass walls is not an ideal shape for a pulsed pressure vessel. Therefore chamber bodies have been quite heavy and rigid to overcome pressure stresses and to reduce the motion between the glass and the chamber. The chamber material must have high strength and good ductility at low temperature, because of the impact load caused by the pressure pulses during

normal operation. High electrical resistivity at low temperature is desirable to reduce eddy-current forces, which occur when magnet power fails and the magnetic field collapses. The permeability of the chamber must remain constant and below about 1.05 throughout the temperature range, to reduce distortions in the magnetic field.[25]

The materials used for the large chambers were aluminum alloy on the 60-inch British chamber (Fig. 21) and stainless steel alloy on the 72-inch Berkeley chamber, the 80-inch Brookhaven chamber, and the 2-meter CERN chamber. Both materials have performed successfully. The advantage of aluminum is that it is nonmagnetic, has a high-thermal conductivity and has a lower cost; its disadvantage is that the physical dimensions of the chamber are large because of its low elastic modulus and lower strength. The larger dimensions require an increase in the volume of the magnetic field. The lower electrical resistivity of aluminum alloys at low temperature requires that the chamber be supported to withstand higher eddy-current forces when electrical power fails.

Stainless steel, although expensive, has higher low-temperature strength and is more rigid. However, its initial low-temperature magnetic permeability must be carefully controlled; and further, it must remain nonmagnetic when exposed to low temperature—for lifetimes of several years. It must not be effected by the temperature cycling between room temperature and liquid hydrogen temperature.

Magnetic measurements are most easily made at room temperature and are usually made to absolute values of 0.1%. The measured values of magnetic field are used for computing momenta, and the accuracy of the computation depends upon how well the magnetic field is known. When the magnetic properties of the chamber metal are stable and the permeability

has an average value less than about 1.005, the effect on the magnetic field can usually be ignored.

The Berkeley 72-inch bubble chamber has a 6 300-lb casting made of austenitic stainless steel similar to AISI 316.[26] Two chemical analyses, shown in Table I, were made to indicate the homogeneity of the casting. A low-temperature permeability test made of samples taken from the casting indicated a value of less than 1.004 from 300 to 20°K. Another room-temperature test with a different sample was measured at 1.0055. It was difficult to weld fittings onto this stainless steel casting because of the poor high-temperature strength of the weld.[27] Weld design is very important when metal with poor high-temperature strength properties must be used.

The Brookhaven bubble chamber body was cast of Kromarc-55, a very weldable high-manganese stainless steel developed by the Westinghouse Corporation. The specification for the Kromarc is shown in Table II. This table also gives the specification for the CERN bubble chamber body.

The stainless steel must remain austenitic to be paramagnetic, and therefore the amount of ferrite and martensite, which are ferromagnetic, must be kept very low. The Schaeffler constitution diagram for stainless steel[28] (Fig. 22) shows that the selected steels used for these large chambers all lie in the austenitic region; this is a very useful way to compare stainless steels for this purpose at room temperature.

Austenite is a face-centered cubic structure that may transform to ferrite, a stable-bodied cubic form, or to martensite, a metastable tetragonal form. Phase changes of this kind are irreversible and may occur when the chamber temperature is reduced. The ferrite transformation is a diffusion process and is essentially complete at room temperature. Observations at room temperature will establish the effect of ferrite on the permeability at room temperature and at lower temperatures.

The transformation from austenite to martensite, however, is a shear mechanism and occurs very fast once the martensite start temperature, M_s, is reached. This effect is described in Reference 29. The bubble chamber operating temperature is above the M_s temperature of the stainless steels listed in Table II in all cases, which indicates that these steels will not transform to martensite. The martensite deformation temperature, M_d, is the temperature at which austenite will transform to martensite as a result of strains that occur in operation. The magnitude of this effect is dependent upon the stress pattern in the casting. Kromarc is the only metal on Table II that is free from this phenomenon, because of its very low M_d temperature.

There is also an upper limit to the amount of nickel that can be added. A reversible change in permeability can occur if very large amounts of nickel are added, say over 50%. In this case, the Curie point is raised above the chamber operating temperature; the chamber will become magnetic when it is cold and return to the paramagnetic state when it is returned to room temperature.

CHAMBER WINDOW

The 5-inch-thick optical window that covers the 72-inch bubble chamber was cast of borosilicate crown glass; at that time it was believed to be the largest piece of optical quality glass ever cast. The window is tilted 7-1/2 degrees from the horizontal to prevent light from reflecting into two of the camera lenses and to allow any hydrogen bubbles collecting under it to roll out of the field of view (where they can be condensed).

For optical quality the specification limited the inclusions to not over five .03-inch bubbles in any square inch of projected area and required that the striae be grade D or better, in accordance with Specification JAN-G-174,

with an index of homogeneity of 0.0001. The window is required to withstand a differential pressure between an external high vacuum and a maximum internal pressure of 150 psi in the chamber. The window temperature is that of liquid hydrogen. The window opening is 20 inches wide by 72 inches long. Strength calculations placed the thickness near 5 inches for untempered glass.

Optical glass was considered and a borosilicate selected. The specific type is BSC-517/645. Selection of this particular type was on the basis of minimum dispersion, high coefficient of expansion compared to other optical glass (about one-half that of the chamber metal), and a belief by manufacturers that this type could be cast in the thickness desired and still meet the bubble and striae specifications mentioned above. This type has previously been used for large-diameter optical windows in wind-tunnel installations.

The National Bureau of Standards (NBS) Cryogenic Engineering Laboratory conducted an experimental investigation to supplement the existing information on the strength properties of BSC-517/645. Information on the strength and fatigue of this glass at low temperature (20°K) was obtained and has been reported.[30] This information was used to compute the window thickness needed to withstand the chamber internal pressure.

Several interesting facts resulted from the NBS testing of BSC-517/645 glass. The strength of the glass, defined in terms of the stress required to cause fracture, increases with decreasing temperature. At 20°K and 76°K the breaking stress is independent of the rate of loading; at higher temperatures there is a dependence on the rate of loading. Contact with liquid hydrogen does not appear to adversely affect the breaking stress.

The fatigue of glass, defined as the decrease in breaking stress with increasing duration of load, decreases with decreasing temperature but still

exists at 76°K. The fatigue limit appears to be greater than 9 000 psi for BSC-517/645 (Table III). At these low temperatures glass exhibits very little or no fatigue and higher design stresses can be used for glass in cryogenic applications.

Glass fails only in tension at the surface. Cooling the window causes temperature differentials that cause differential contraction and place the glass surface in tension. Thus the cooling rate is determined by the permissible tension stress. The strength tests showed that the probability of failure was less than 1% when the glass was stressed to 9 000 psi in tension, and from this data a design stress of 2 000 psi was selected.

After selection of the design stress, the maximum permissible temperature difference in the glass (ΔT) can be calculated from[31]

$$\Delta T = \frac{(1-\mu)S}{\alpha E} ,$$

where

μ = Poisson's ratio,

S = stress,

α = expansion coefficient,

E = Young's modulus.

This curve is shown in Fig. 23. The permissible ΔT curve is hyperbolic because the coefficient of contraction decreases with temperature. At about 110°K, liquid nitrogen can be put into contact with the glass, because the temperature difference between the liquid nitrogen and the glass (33°K) equals the glass permissible ΔT for 2 000 psi.

After the permissible temperature difference has been determined, the allowable heat flux can be calculated. The process for cooling the glass determines from which surfaces heat is removed. The glass on the 72-inch bubble chamber is cooled by natural convection, which makes the chamber

operation less complicated. A 5-psig atmosphere of hydrogen or helium gas surrounds the glass during cool-down and couples the glass to the heat-exchange surfaces located above and below the glass. The heat exchangers are cooled by the refrigeration system.

The top surface of the glass is cooled more efficiently than the bottom surface because a natural convection circuit exists, consisting of the "hot" glass surface; the cold walls; and the radiation shield, at the top, which is at the temperature of the refrigerator. Inside the chamber the effectiveness of a natural convection circuit to cool the bottom of the glass was in doubt. Therefore it was assumed in these calculations that the glass would be cooled from the top side only, and that any cooling from the bottom side would be "safety factor" and would compensate for errors in measuring the glass surface temperatures.

The allowable heat flux, q, was calculated from the expression

$$q = \frac{2k\Delta T}{t} ,$$

where k is the thermal conductivity corresponding to the temperature of ΔT and t is the glass thickness. By substituting the expression for ΔT, we obtain

$$q = \frac{2k(1-\mu)S}{t\,\alpha\,E} = (\text{constant})\ \frac{k}{\alpha} .$$

Also, k/α is nearly constant between $100^{\circ}K$ and $300^{\circ}K$, $q = 0.28$ W/in.^{2}.

The maximum permissible cooling rate may be determined by calculating the cooling surface area and the total heat content of the glass area, and by knowing the allowable heat flux. A minimum cool-down time of about 24 hours or a rate of $9^{\circ}K/h$ is obtained, assuming that the temperature gradient on the surface of the glass is zero and that all the ΔT is available to transfer heat.

In practice the glass cool-down rate must be corrected when temperature gradients appear on the glass surfaces. The actual permissible temperature difference is the maximum temperature difference between any two points in the glass and includes the gradient through the glass due to the cooling rate plus the surface gradients. Therefore the cooling rate must be reduced when surface gradients appear. The rate correction is

$$\Delta^{\circ}T_{actual} = \Delta^{\circ}T\left[\frac{\Delta T_{max} - \Delta T_{surface}}{\Delta T_{max}}\right], \ ^{\circ}K/h.$$

There is some cooling by radiation but this is not very great because the temperature difference between the metal parts and the glass is kept small during cool-down so that the glass is not locally stressed.

The actual cool-down time required is about 65 hours or about $4^{\circ}K/h$. The 65 hours becomes limited by the refrigerator at lower temperatures, which is a built-in safety feature. The refrigerator and cool-down rate are well matched.

The glass is warmed to room temperature in about 50 hours by circulating hydrogen gas through the refrigerator. The rate is faster on warm-up because the surface of the glass is in compression rather than in tension. The main insulating vacuum can be removed safely when the glass is at about $150^{\circ}K$.

Tempered glass has also been used on bubble chambers. It permits using a reduced glass thickness, which has the advantage of lower cost and faster cool-down. For very large chambers the size of annealed glass may exceed the manufacturing capacity, and tempered glass may be the only choice.

INFLATABLE GASKET

A tight seal must be maintained between the chamber body and the glass window so that an insulating vacuum can be maintained above the glass. On smaller chambers this seal is made quite simply. A lead gasket clamped between the glass and metal chamber by means of bolts is one choice. The chamber is then assembled inside the vacuum tank, and the apparatus is cooled to liquid hydrogen temperature. However, this method did not appear feasible with the large chamber, because the difference in shrinkage between the glass and chamber might cause the seal to open during cool-down. With the 72-inch chamber there is a difference in shrinkage of about 3/16 inch in 72 inches between the glass and metal. On smaller chambers the difference in shrinkage is less, so that the problem of making a seal is simpler.

For smaller chambers, the problem then was to devise a type of seal that could be effected at 27°K. This was complicated by two factors: Lead is so hard at 27°K that it could not be compressed against the glass without producing dangerous stresses in the glass; and once the chamber has been cooled down, all the parts are inaccessible.

These difficulties were overcome by the design of an inflatable gasket[32, 33] (Fig. 24). With this gasket, two thin stainless steel tubes are inflated with high-pressure helium gas. This forces the two gasket blocks apart, compressing indium wires against the contacting surfaces (i.e., the glass window and the chamber). Indium was chosen because it is softer at 27°K than lead is at room temperature. Since the valve controlling the helium inflation gas is accessible, the seal can be made after the cool-down has been completed.

The inflatable gasket, though it gives an adequate seal, does not provide an absolutely tight one. The small amount of gas leaking past the indium wires is pumped off via intermediate pumpouts, which can be seen in Fig. 24.[34]

The helium pressure in the gasket is maintained at 50 psig[25] during cool-down, to hold the glass in position. When the chamber is cold, the inflation pressure is increased to 200 psig to seal the gasket. The chamber is then pressure-tested to an internal pressure of 145 psig (155 psig across the glass) with helium gas. The helium pressure in the gasket is raised as required to make the seal—usually up to 400 to 500 psig.

The seal improves during the first days of operation and has operated successfully and continuously for as long as 10 months (over 2 000 000 cycles) on a single run. The gasket assemblies have been in use 3 years.

Chamber Prestress

When the chamber is pressurized, deflections occur at the bubble chamber glass opening, which, if too large, may cause the inflatable gasket to slip. The deflections due to operational pulsing pressures may cause further slipping, or they may cause the inflatable gasket to roll, which could lead to fatigue failure. To reduce the deflection, the window flange could be made heavier or the chamber could be prestressed with a compressive load through the glass. In the case of the 72-inch bubble chamber it was not desirable to increase the depth of the flange because this would either increase the magnet size or decrease the chamber size. Chamber prestress using a compressive preload through the glass was adopted.

The chamber was assembled and a test performed to determine the amount of deflection during operation. The deflections of the casting were measured at internal pressures up to 70 psig, at which it deflected 15 mils.[35] At the design maximum operating pressure of 120 psig, the casting should deflect 25 mils.

A second test, to determine the reaction force in the glass, was made with only the chamber and hydrogen shield. This measurement was made by applying a point load at the center of the window opening, the prestress load point.[36] The spring rate of the casting is 860 000 pounds per inch, or 33 500 pounds for a 38-mil deflection. This deflection is the amount of the differential expansion between the chamber and the glass across the width. The 38 mils is 13 mils more than the 25 mils required to prevent movement of the chamber during pulsing. The 13-mil margin was selected because it can be obtained simply by putting the glass in contact with the casting through snug-fitting indium pads.[37] The snug fit corresponds to zero prestress at room temperature and simplifies the assembly. The casting is "soft" relative to the glass so that errors in calculating the differential expansion and the fitting of the indium will not cause excessive stress in the glass.

The preloading on the glass is made through $4\frac{1}{2}$-inch by 10-inch grooved indium pads. The glass compressive stress is 744 psi (assuming 100% contact when the casting is deflected 38 mils).

Because of the slow cool-down there may be a creep effect in the indium that at present is unknown. Any creep effect would be in the safe direction, since it will reduce the amount of deflection of the casting and thus reduce the load on the glass. Also, creep in the indium implies an increase in area of contact, which lowers the stress on the glass.

VACUUM SYSTEM

A thermal-insulation system that allows the chamber to be removed easily is more important on research apparatus than a small gain in thermo-efficiency. Radiation shields and super-insulation have been used.

The diffusion-pump speed required for normal operation is very low because the bubble chamber body at 20°K is a very large cryopump.

However, high pumping speeds are needed to overcome hydrogen or helium leaks which cannot be cryopumped at this temperature and which occur particularly when the chamber is kept cold continuously for periods of a year.

Large pumping capacity in the 100-mm range is very desirable. It permits quick recovery during emergency periods and also provides fast pump-downs, particularly during the purging cycles. The vacuum system should be protected against power failures.

The 72-inch bubble chamber is thermally insulated by suspending it inside a vacuum tank. The structure by which the chamber is suspended is called the "hydrogen shield" (Fig. 19). This shield is made of 3/16-inch-thick stainless steel reinforced with a series of ribs. The primary function of the hydrogen shield is to serve as a protective enclosure for the chamber in case the glass window should break or the inflatable gasket fail. Liquid hydrogen expanding into the hydrogen-shield enclosure would rapidly boil. To keep the pressure from rising to a dangerous level, a safety-vent system has been installed (Fig. 25). If the pressure in this enclosure should rise above 25 psig, a relief valve would open. The gas would then escape into a 22-foot-diameter steel sphere located in a remote area. During normal operation this sphere is kept evacuated.

The hydrogen shield contains a liner that is cooled to liquid hydrogen temperature. The purpose of this liner is to intercept most of the thermal radiation coming from the cover plate of the vacuum tank, which is at room temperature. If this heat were allowed to impinge on the glass, bubbles would form underneath it, and an unwanted temperature gradient would be introduced in the chamber liquid.

NITROGEN SHIELD

The nitrogen shield is a 1/4-inch-thick copper tank suspended from the sides of the vacuum tank. This shield surrounds the chamber on its sides and bottom and is cooled with liquid nitrogen (77°K). It acts as a thermal radiation barrier, helping to prevent heat from reaching the chamber from the vacuum tank, which is at room temperature.

EXPANSION SYSTEM

The chamber liquid may be expanded many different ways, such as:

1. Gas expansion
2. Free piston
3. Driven piston
4. Bellows
5. Diaphragm
6. Moving window .

The so-called gas expansion is described below for the 72-inch bubble chamber. The chamber and expansion line operate at about 5 atmospheres pressure with hydrogen and about 6 atmospheres with deuterium. The expansion system for the 72-inch bubble chamber was designed for 10 atmospheres, which is marginal protection against the constant pulsing. A design pressure of 20 atmospheres and as much vibration protection as possible would be more desirable for the expansion line, the refrigeration, and other tubing inside the vacuum tank.

The expansion system is shown schematically in Fig. 25, together with a simplified schematic of the refrigeration, vacuum, and safety-vent systems. The liquid hydrogen in the chamber is held at 82 psig by a column of hydrogen gas in the expansion line. Opening of the expansion valve allows this gas to expand into the expansion tank, which is maintained at 5 psig.

When this occurs, the pressure in the chamber drops from 82 to 45 psig in about 10 msec. During this brief interval the particle beam is introduced and a photograph taken, as described earlier. In the meantime the recompression valve has been opened and the expansion valve closed. Hydrogen gas at 115 psig then flows from the recompression tank into the expansion line. The chamber pressure rises rapidly, slightly overshooting its original value of 82 psig, and then levels off at 82 psig (Fig. 13).

The line length and diameter of the expansion line were selected to give a minimum heat loss for normal operating conditions. Minimum heat loss is obtained by bringing the minimum amount of cold gas into the room-temperature part of the expansion line.

The total time for expansion and recompression is about 20 msec. This cycle is repeated 11 times each minute. Hydrogen gas in the expansion tank is pumped continuously through a purifier and into the recompression tank by the recompression compressor. Since this gas comes in direct contact with the chamber liquid, it must be very clean. The constant circulation of hydrogen gas from the expansion tank to the recompression tank can "pump" contaminants from the compressor into the chamber so that after a long period of time contaminants can build up in the chamber. A bubble chamber purification system must be much better, for example, than one used in an ordinary liquifier used to fill dewars, where the gas is pumped only once through the compressor, and the contaminants are carried away in the dewar with the liquid.

Fast recompression is essential for maintaining a uniform temperature throughout the liquid by compressing bubbles out of existence before they can rise appreciably from their point of origin. However, fast recompression also helps maintain this uniform temperature in another way. Before the

liquid has a chance to evaporate in the expansion line it is forced back into the chamber. Only a small amount of mixing occurs in the expansion line, so that the upper portion of the line remains nearly at room temperature, while the lower end stays at 27°K. Because the upper portion is at room temperature, refrigeration does not have to be provided around the expansion and recompression tanks. Also, the expansion and recompression valves can operate near ambient temperature.

During the expansion cycle the liquid hydrogen expands up to 1.8% of the total volume (about 9 liters),depending upon the temperature. This liquid flows out of the chamber into the lower expansion line. During recompression this same liquid flows back into the chamber. If this flow occurred at one end of the chamber, considerable turbulence would result, which would distort the tracks and reduce the value of the photographs. To minimize turbulence, this flow is directed through two expansion plates, one on each side of the chamber (Fig. 26). Many small holes are drilled in each plate. The liquid flows out through these holes into a collecting manifold that is connected to the expansion line. The liquid is returned through these holes on recompression. The expansion plates also function as heat exchangers and are cooled by evaporating coils that are attached to the expansion plate and connected to the refrigerator. The liquid is cooled when it passes through the heat-exchange holes in the expansion plates.

The liquid thermal gradients and optical distortion are greatly reduced by a circuit that introduces liquid hydrogen (rain, as it is called) at the gas - liquid interface in the expansion line[38] (Fig. 27). This system supplies the major portion of refrigeration to the chamber. The injection is accomplished through an auxiliary filling circuit connected in such a way as to keep the mass of hydrogen constant. Gas is bled from the recompression tank, through a liquid nitrogen recool, into a heat exchanger that

counterflows with refrigerant entering the system, and finally through a 5-μ stainless steel filter into the expansion line. Approximately 7 grams per pulse enters the line through the fill pipe located about 30 cm above the static liquid level. It is important that both valves shown in Fig. 27 be well-throttled in order to decouple an inherently unstable loop. The throttled valves prevent the pressure variations in the recompression tank and expansion line from unbalancing the flow through the heat exchangers during the 30-msec pulse.

The effect of this technique is twofold. The counterflow heat exchanger and the side plates now share the refrigeration load in about equal proportions; this results in lower gradients in the chamber and closer coupling to the refrigerant. Secondly, the cooling of the interface suppresses vaporization and therefore reduces liquid thermal gradients in the line. Thus the total thermal inhomogeneity of the system is reduced, in turn effecting a reduction of distortion and density fluctuations.

The resulting change in picture quality is dramatic and permits a threefold increase in pulse rate. Previously the chamber bottom was filled with a shimmering turbulence which now appears only near the expansion end. Temperature gradients in the visible liquid are halved to less than $0.15^{\circ}K$. Most important, interface cooling increases the available sensitive volume 25% by making the bottom 3 inches of the chamber usable.

The two identical 6-inch boot valves used to expand and recompress the pressure in the 72-inch bubble chamber[39] are similar in design to the Grove Company Flexflo Model 80 valve, which uses a rubber boot over a slotted aluminum core (Fig. 28). The valve opens in 6 to 10 msec, with hydrogen gas. The expansion valve is opened just long enough to reduce the chamber pressure and to minimize the amount of cold gas passing

through the valve (about 25 grams per pulse). When cold gas flows through the valve too long, the life of the rubber boot is reduced. Warming coils have been added on the boot valve to increase the bulk temperature.

The boot life is about 150 000 cycles for the expansion valve, which has the cold gas flowing through it. The recompression valve boot life is over 2 000 000 cycles. The pulsing of the rubber boot has a hysteresis heating effect which helps warm the boot.

Other large bubble chambers now under construction use either gas expansion, driven-piston expansion, or free-piston expansion. The piston expansion system has a piston in contact with the liquid hydrogen. This piston is driven by a gas-actuated piston at room temperature.

The free piston is a modification of the gas expansion system and has a light-weight piston in the gas column, with one end in contact with the liquid hydrogen and the other end at room temperature. The temperature gradient is taken through the light-weight piston. The piston is driven by energy from the compressed liquid hydrogen. The free piston prevents warm gas from mixing with cold gas; this system is expected to be more efficient.

Another modification of the piston system is a chamber with a bellows mounted in the body of the chamber (Fig. 29). This arrangement allows one side of the chamber to move — in this case a moving window. The energy for the expansion is supplied by the compressed liquid hydrogen in the chamber. Such a design should give low temperature gradients and turbulence in the field and require a minimum of refrigeration. This system will be used in a 25-inch-diameter hydrogen bubble chamber now under construction at the Lawrence Radiation Laboratory.

The main advantage of the gas expansion system is that it does not have any moving parts at low temperature or inside the vacuum tank. Expansion valves can be changed without emptying the chamber. However, this system is more inefficient and may cause higher turbulence in the chamber.

Piston or bellows expansion systems have the disadvantage that the chamber must be emptied and warmed to room temperature in the event the cold piston requires repair. Piston-type expansion has been very reliable and is more efficient with less turbulence.

The choice of expansion system should be made on the basis of turbulence required and chamber reliability.

The size of the refrigerator for large chambers is usually determined by the time required to cool the glass and the chamber. It would be desirable to match the cool-down power requirement to the pulsing refrigeration power requirement. In any case the electrical input power to the refrigerator is small, and the savings here is small when compared to the input power of 2 to 7 megawatts required to energize the bubble chamber dc magnet.

MAGNET

The 72-inch bubble chamber magnet contains 115 tons of steel in its core and about 20 tons of copper in its exciting coils. Current is supplied to the magnet coils by two series-connected motor generators. These generators operate at 4600 A, 550 V, giving a power output of 2.53 magawatts. The heat produced in the coils is dissipated by cooling water flowing through the hollow copper conductor. The total number of ampere-turns is 1.74 million, which gives an 18 000-gauss field at the center of the chamber.

The magnet current is regulated so that fluctuations in the magnetic field do not exceed 0.03%. Constancy of the field with time is necessary to permit accurate determination of particle momentum. Further, the magnet was designed so that the flux distribution in the region of the chamber would be uniform within 15%. These variations (which do not vary with time) are compensated for mathematically when the tracks are analyzed by a computer.

Magnet Walking System

The 72-inch bubble chamber was designed so that it can be moved from one location to another around the Bevatron for different experiments. It was not feasible or necessary to transport all the auxiliary equipment; the large compressors, the motor generators, and some of the vacuum pumps are installed in permanent locations. Connections are made to this equipment after the chamber has been moved.

Two of the four "feet" used to walk the bubble chamber can be seen in Figs. 10 and 20. Each foot is equipped with two hydraulic cylinders, one for vertical motion and one for horizontal motion. For the magnet to walk, the feet push downward, lifting the magnet. While the magnet is raised, it is pulled horizontally. The magnet then lowers until it again rests on its center supporting structure. The feet then rise and reset forward. As this cycle is repeated, the magnet assembly (which weighs about 240 tons) is moved about 1 foot each step, with an average speed of 70 ft/h.

Because the chamber is placed in a vertical magnetic field, particles entering through the fringing field are deflected in the horizontal plane. Since the long direction of the chamber is horizontal, it is necessary to rotate the chamber about a vertical axis for accurate alignment with the direction of the beam. This alignment can be accomplished by rotating the magnet assembly about its own geometric center.

Photographic System

In order to determine track curvature in three-dimensional space, it is necessary to use stereo photography. The tri-stereo camera is shown in Fig. 30 (the optical layout was shown in Fig. 4.). The lenses (1, 2, and 3) are located at the vertices of a 45-degree right triangle, giving three stereo pairs of photographs (between 1 and 2, 2 and 3, and 1 and 3). One stereo axis (2, 3) is parallel to the beam direction and the other (1, 2) is perpendicular to it. When measuring photographs, one chooses the stereo pair whose axis is most nearly perpendicular to the track direction. This allows more accurate measurement of the dip of a track.

The stereo camera uses a magazine containing 1 000 feet of 46-mm film. The film is automatically advanced after each exposure.

Illumination is provided by three xenon-filled flashlamps (strobe lights) mounted in a projector above the stereo camera (Figs. 30 and 4). The film is exposed by firing these flashlamps, rather than by opening and closing a shutter. This method gives an effective exposure of about 250 μsec. Exposure must be completed within a few milliseconds after beam passage, before the bubbles grow too large or move appreciably from their point of origin. The timing of each flash is automatically controlled to occur about 2 msec after the beam enters the chamber (Fig. 13).

The dark-field illumination system is similar to that developed for the 15-inch chamber, except that a larger number (111) of optical retroreflectors span the chamber bottom, as shown in Fig. 4.

TRACKS AND BUBBLE SIZE

The primary beam from the accelerator is controlled to admit about 10 particles per pulse into the chamber. The number of tracks in a picture varies according to the experiment, but too many tracks make it difficult to identify and measure the nuclear event to be studied. The bubble density along the track is usually about 15 bubbles per centimeter.

The diameter of the bubbles forming the track is controlled by changing the time between beam injection and the camera light flash. The time delay is within a range of 3 msec, and gives a bubble of about 0.3 to 0.5 mm in diameter.

Bubble size as used herein means the actual diameter of the bubble at the time the picture is taken. However, it has also been used to mean the image diameter on the film times the magnification, which may not be an indication of the true bubble diameter because of defraction effects of the lens, characteristics of the film emulsion, and also the diameter of the light reflection on the bubble.[40, 41]

SECTION IV

BUBBLE CHAMBER REFRIGERATORS

BUBBLE CHAMBER REFRIGERATORS

For successful operation, liquid hydrogen bubble chambers are conventionally operated at a temperature near 27°K. To maintain the desired operating temperature, refrigeration must, of course, be provided to intercept heat transferred to the chamber from the environment and to absorb the energy input to the chamber liquid due to pulsing.

In principle, this refrigeration can be provided by evaporating either liquid hydrogen or liquid neon. It would also be possible to absorb the heat by warming a helium gas stream that had previously been cooled to some lower temperature in a suitable refrigeration process. Refrigeration is provided at appropriate parts of the bubble chamber by use of suitable heat exchangers to transfer heat from the chamber liquid to the refrigerant.

In the early stages of liquid hydrogen bubble chamber development, the necessary refrigeration was provided by the evaporation of liquid hydrogen from a vented reservoir. These chambers ordinarily contained only a few liters of liquid hydrogen. It was obvious that when considering both economics and safety, larger chambers should be refrigerated with some type of closed-cycle system. Since liquid hydrogen is used in the chamber, there should be no additional complication or danger resulting from the use of a closed-cycle hydrogen refrigerator. Such a refrigerator can also be designed to operate quite reliably.

Before describing hydrogen refrigerators that are either in use or planned for use with specific liquid hydrogen bubble chambers, it is instructive to consider the desirable qualities of a closed-cycle refrigeration system. These qualities can be seen by considering their effect on economics, logistics, and safety.

The use of a closed-cycle process is a more economical method of providing refrigeration than the evaporation of liquid from a vented reservoir. Venting of the reservoir to the atmosphere results not only in the loss of hydrogen gas formed by liquid evaporation, but also in the loss of the refrigeration in that gas. In contrast, a refrigerator operating on a closed cycle uses the refrigeration available in the gas formed by liquid evaporation. Since the sensible heat of 1-atmosphere hydrogen gas from the saturation temperature to ambient temperature is eight times the latent heat of vaporization, this refrigeration effect is quite significant. In fact, the use of this refrigeration reduces the power required to operate a refrigerator to nearly one-half of the total power required to operate a liquefier for equal quantities of refrigeration.

For bubble chamber refrigeration needs, this difference in power requirement may not be of major economic importance, since other factors, such as labor, predominate. However, the power requirement influences the capital cost significantly, since the compressor cost is proportional to compressor power and may be about one-third of the total refrigerator cost.

The cost of commercial liquid hydrogen produced in tonnage plants using inexpensive sources of hydrogen gas must be considered when analyzing the economic feasibility of the purchase and operation of a closed-cycle refrigerator. The losses incurred in storing and handling commercial liquid hydrogen must, of course, be considered in such an analysis.

The use of either liquid hydrogen produced in an adjacent liquefier or commercial liquid hydrogen, requires dewars and transfer systems to support a bubble chamber refrigeration requirement. Thus the safety problem is increased, since each handling enhances the possibility of introducing contamination into the dewars. Perhaps a more serious factor is the

likelihood of hydrogen escaping into the surrounding area; consequently, access to the container storage area should be controlled.

Several liquid hydrogen bubble chambers have been either completed or planned that use a closed-cycle hydrogen refrigerator to maintain the chamber temperature constant. Some of these refrigerators are described below. In addition a system using helium gas as a refrigerant is mentioned. No attempt is made to furnish detailed engineering design information, however references are given where it seems appropriate.

REFRIGERATOR FOR 72-INCH LAWRENCE RADIATION LABORATORY HYDROGEN BUBBLE CHAMBER

A closed-cycle refrigerator using hydrogen as the working fluid was chosen.[42] The refrigerator was designed to produce 1800 watts at 27.5°K with a circulation rate of 200 standard cubic feet of hydrogen per minute. Figure 10 shows a photograph of the bubble chamber installation. The refrigerator is controlled from the panel board shown at the left of the photograph. Figure 31 is a simplified schematic of the refrigeration system used. This refrigerator has operated several thousand hours with only routine compressor maintenance being needed.

Process

The simple Linde process, using liquid nitrogen for precooling, was selected because of high reliability. Hydrogen is compressed to 150 atmospheres, then oil and water are removed in adsorption purifiers that are maintained at ambient temperature. Since the refrigerator can also be used as a hydrogen liquefier, an additional refrigeration drier-purifier is provided to remove trace impurities of nitrogen, oxygen, and carbon dioxide which may be present in electrolytic hydrogen gas used for liquefaction.

After purification, the compressed hydrogen gas is cooled in counterflow heat exchangers by the low pressure gas being returned to the compressor intake. Liquid nitrogen is used to further cool the incoming compressed hydrogen gas. Further cooling takes place in the final or Joule-Thomson heat exchanger, and in expansion through a valve. Approximately 50% of the gas is liquefied during the expansion process, and refrigeration from the latent heat of vaporization is available to the bubble chamber. After this refrigeration has been removed, the saturated vapor is returned to the compressor intake through the low pressure side of the counterflow heat exchangers to complete the cycle.

Refrigerator Control

The temperature of the liquid hydrogen in the LRL 72-inch bubble chamber is controlled by simultaneously modulating the temperature and mass flow rate of the refrigerant. Figure 31 shows the essential components of the control system. Valve 1 maintains a preset operating pressure to the refrigerator, bypassing excess flow to the compressor intake.[42] Valve 6, the conventional refrigerator expansion valve (valve 5 closed), is used in this case as a mass flow valve and therefore determines the quantity of refrigeration. Valve 7 determines the temperature of the refrigeration by controlling the vapor pressure of the refrigerant. Input to the flow and temperature control come from vapor pressure thermometers VPT-1, VPT-2, and VPT-3.

Operation of the control system can be shown by referring to Fig. 32. Compressed hydrogen gas is cooled in the final heat exchanger to point A, then is expanded and further cooled through flow control valve 6. The resulting mixture of liquid and gas enters the evaporator at point B. Most of the refrigeration is accomplished by nearly isothermal evaporation of the liquid

as it passes through the evaporator. To assure complete evaporation of the liquid and thus prevent an accumulation of liquid in the refrigerator evaporator, the fluid is slightly superheated (to point C) before returning to the refrigerator. This slight superheat is maintained by the action of flow control valve 6, which responds to changes in a preset temperature difference or the degree of superheat between the inlet and outlet of the evaporator.

Valve 7 is controlled by the temperature of the bubble chamber liquid, and the refrigerant temperature is thereby controlled according to refrigerator load.

The heat exchanger, E, located at the low-temperature end of the evaporator is needed to evaporate liquid that might be carried over from the evaporator during changes in the refrigeration requirement. The normal superheat of the returning refrigerant is sufficient to evaporate liquid accumulated at E.

Novel Features

The LRL refrigerator for the 72-inch bubble chamber uses a more effective heat-exchanger design than has previously been reported in the literature for Hampson-type heat exchangers. This novel feature is a variation in the radial spacing between tube layers. This makes it possible to match the low-pressure flow outside the tubes to the high-pressure flow inside the tubes. Thus the refrigeration available in the low pressure gas is distributed in proper proportion across the entire heat exchanger. Correlations for this heat exchanger are given in Reference 42.

REFRIGERATOR FOR BRITISH NATIONAL BUBBLE CHAMBER PROGRAM

The refrigerator built for the British National bubble chamber (BNBC) program uses the same process as the LRL 72-inch bubble chamber refrigerator. The capacity is somewhat larger, being designed to produce slightly more than 3 000 watts at 27.5°K, with a circulation rate of 400 standard cubic feet of hydrogen per minute. Figure 33 is a photograph of the bubble chamber control board. The control valve assembly and a simulated refrigeration load are shown in the foreground.

The BNBC refrigerator control system is multizoned. The zones are in parallel and can be operated at different temperatures and refrigeration loads. Multiple zones are possible by providing parallel control systems. Referring to Fig. 31, valve 6, the evaporator and valve 7 are provided in parallel for a multiple-zone control system. In addition, valves 6 and 7 are interconnected in the control system through a pneumatic additive device that senses sudden load changes and operates both valves immediately. This anticipatory control eliminates the time lag found in the LRL control circuit.

Hampson-type heat exchangers are used in the refrigerator, incorporating the same novel spacing feature as in the LRL refrigerator.

REFRIGERATOR FOR 80-INCH BROOKHAVEN BUBBLE CHAMBER

A closed-cycle hydrogen refrigerator has been built recently for operation with the 80-inch Brookhaven hydrogen bubble chamber. The Linde process is also used for this refrigerator. A capacity of 2 600 watts at 25°K has been specified using liquid nitrogen as a precoolant at 80°K and a hydrogen circulation rate of 400 standard cubic feet per minute. If additional refrigeration is needed the precooling temperature can be lowered by reducing the pressure over the liquid nitrogen precoolant. The capacity is then estimated to be 3 800 watts.

This refrigerator differs from the LRL and BNBC refrigerators in that it is completely-self contained. That is, the liquid nitrogen needed for purification, precooling and other miscellaneous uses is provided by a closed-cycle refrigerator located adjacent to the hydrogen refrigerator. In addition, precooling to increase the efficiency of the nitrogen refrigerator is provided by a closed-cycle freon refrigerator. Figure 34 is a photograph of the completed refrigerator.

Multiple temperature-control zones are also being planned in this application.

REFRIGERATOR FOR 15-INCH LAWRENCE RADIATION LABORATORY BUBBLE CHAMBER

The simple Linde process, using liquid nitrogen for precooling, was also used in a 300-watt, 27°K refrigerator built to continuously refrigerate the 15 inch LRL liquid hydrogen bubble chamber.[43] In fact, this refrigerator is quite similar to the one built for the LRL 72-inch hydrogen chamber. Figure 35 shows a schematic arrangement of the refrigeration system and Fig. 36 shows a photograph of the refrigerator installation.

Refrigerator Control

It is seen that the control system is different from that of the refrigerators mentioned above. The method selected for control of this refrigerator depends on pressure control. Gas pressure in the high-pressure circuit is maintained constant by varying the compressor bypass valve, PCV-3, and the main refrigerator expansion valve. A variation in the refrigeration rate is reflected in the liquid hydrogen evaporation rate. This directly affects the pressure in the low-pressure circuit, and valve PCV-3 acts to maintain the compressor intake pressure fixed. For instance, a reduction in the refrigeration load tends to reduce the pressure in the low-

pressure circuit, and valve PCV-3 opens to keep the compressor intake pressure constant. This action of PCV-3 tends to reduce the compressor discharge pressure; however, this tendency is transmitted to a controller which closes the expansion valve proportionally. This action maintains the discharge pressure constant and reduces the flow to the refrigerator. An increased refrigeration requirement produces a similar sequence of events and results in increased hydrogen flow through the expansion valve while maintaining the compressor discharge pressure constant.

REFRIGERATOR FOR CERN 2-METER HYDROGEN BUBBLE CHAMBER

A closed-circuit hydrogen refrigeration plant having a capacity of 4 000 watts at 23°K is planned to refrigerate the CERN 2-meter hydrogen bubble chamber. A low-pressure cycle using turbine expansion engines is being constructed and is described in Reference 44.

Process

Figure 37 shows a schematic arrangement of the process. According to Reference 44 hydrogen gas is compressed in a two-stage oil-free labyrinth-piston compressor to a pressure of 8 atmospheres. Cooling takes place in the main counterflow heat exchanger, 2, after which the gas stream is divided. The main flow is expanded in two turbines, 3 and 4, connected in series, and exhausts to a final pressure of 1 atmosphere. This gas is returned to the compressor intake through the condenser, 5, and the main counterflow heat exchanger. A secondary flow is liquefied in condenser 5 and collected in reservoir 6. This liquid is expanded and used for cooling the bubble chamber. Complete evaporation and slight superheating occur in the chamber cooling system. The superheated gas then mixes with the gas coming from the turbines and returns to the compressor intake.

Figure 37 also shows the system for charging the refrigerator and chamber with gas. This is described in detail in Reference 44.

Figure 38 is a photograph of the completed refrigerator.

Refrigerator Control

The refrigerator is controlled by maintaining the pressure in reservoir 6 constant by regulating bypass valve 8. The refrigeration available is governed by throttle valve 9, located ahead of the expansion turbines.

Novel Features

As was stated above, this refrigerator uses turbines to produce the necessary cooling. The turbines are supported on oil-lubricated bearings of the journal type, and are designed for speeds in excess of 100 000 rpm. The diameter of the rotors is 60 mm, and they are mounted on a shaft extending into the cold region. The refrigerating capacity of a single turbine operating at a reduced pressure ratio is sufficient to take the static load of the chamber.

REFRIGERATOR FOR 40-INCH BUBBLE CHAMBER AT CAMBRIDGE ELECTRON ACCELERATOR

The 40-inch hydrogen bubble chamber at the Cambridge electron accelerator is to be refrigerated by a system completely different from the refrigerators described above, in that helium is used as the refrigerant.

Helium is compressed from 50 to 550 psia in a three stage reciprocating compressor. Aftercoolers on each stage condense lubicating oil, which is partially removed in a mechanical type separator. Complete oil separation is accomplished in a chamber where the helium is cooled to about $-20^{\circ}C$ and the oil is condensed. The pure high-pressure helium then is cooled in a counterflow heat exchanger and finally expanded in a reciprocating engine where it is further cooled to $20^{\circ}K$. The expanded helium

then enters the bubble chamber condenser where the hydrogen refrigeration takes place. After the condenser, the helium, which has been slightly warmed, is returned to the compressor intake through the counterflow heat exchanger.

This refrigerator is designed to produce 1 500 watts at 20°K. The refrigeration capacity can be varied by changing the pressure ratio across the expansion engine. To insure high reliability there are parallel heat-exchanger and expansion-engine systems, each capable of delivering the required refrigeration.

OTHER BUBBLE CHAMBER REFRIGERATORS

Two other refrigerators for use with hydrogen bubble chambers deserve mention. Both are modified versions of the system previously described for use with the 15-inch LRL chamber. One is for the Midwestern Universities Research Association (MURA) and has a capacity of 500 watts at 27°K. The other is used to refrigerate the 30 inch Columbia University chamber. Metal-diaphragm compressors are used with the Columbia refrigerator.

SECTION V

OPERATION AND COST

GENERAL OPERATION

The installation and operation of a cryogenic bubble chamber is as important as the design and construction. Emphasis must be placed on safety. If an awareness of the potential hazard of liquid hydrogen is present from the beginning, the system will be safe and also reliable. The bubble chamber can be considered as a system made up of the following:

1. The design and fabrication of the chamber
2. The installation, including the building and safety devices
3. The operation.

The definition of "safe" is difficult to state, but in an effort to be safe the system should not become so complex that it is actually unsafe. The choice should be toward simplicity — well-marked panels and piping, and the use of written procedures and guidelines.[45] Safety in the handling and storage of liquid hydrogen are covered in another section of this book.

The 72-inch bubble chamber has three levels of electrical safety interlocks and emergency procedures:

1. A pressure of 1 psig in the main insulating vacuum tank is the highest level alarm, and signals that the chamber insulation has been lost because the interlock is set one pound above atmospheric pressure. The alarm also indicates that the tank is filled with gas. This interlock removes all power and isolates the hydrogen-gas and vacuum system.
2. Electrical power failures, which occur unexpectedly about twice a year.
3. Many lower-order emergencies are on an interlock system that causes the chamber to stop pulsing.

The crew chosen to operate hazardous research apparatus must have the engineering knowledge to make fast accurate decisions and the leadership qualities to act on them quickly. These abilities are also required to obtain high operating efficiency because only one model of a complex research apparatus is usually constructed, so that the prototype becomes an analogue for its own new developments.

Operation of the 72-inch bubble chamber requires 5 men: the crew chief and one man operating the chamber, two men in the compressor room, and one man for liaison and monitoring the beam path between the accelerator and the chamber.

The bubble chamber is available for physics experiments 90% of the time, with 4% lost for film change, 2% lost for expansion system maintenance, and 4% for all other reasons. An experiment lasts from 3 months to a year, and the chamber is pulsed over 2 000 000 times in a year. The newer chambers operating with accelerators having faster pulse rates will be pulsed very much faster.

The 72-inch bubble chamber required four years to develop, design, and construct. About 65 man-years of effort by Laboratory personnel plus outside contracts went into this effort. The total cost of the project, including the building, was about $2 000 000.

The time required to construct various bubble chambers in the past is shown on Fig. 39 and their cost on Fig. 40. The chambers that were constructed in short times usually have higher costs. The construction time is the elapsed time from the decision to build until the first pictures are taken with an accelerator beam. This data is historical and does not compensate for the fact that different groups used or had a different number

of people available for engineering, whether or not construction was started early or went through a long study period, and differences in expenses between different countries.

REFERENCES

1. Alvarez, Luis W., The Bubble Chamber Program at UCRL, University of California Radiation Laboratory Internal Report, April 1955 (unpublished).

2. Calhoun, E., The 72-inch Bubble Chamber, Lawrence Radiation Laboratory Publ. No. 31, July 1960 (unpublished).

3. Glaser, Donald A., The Bubble Chamber, Handbuch der Physik (Springer-Verlag, Berlin, 1958), Vol. 45, p. 314.

4. Alvarez, Luis W., Liquid Hydrogen Bubble Chambers, in Experimental Cryophysics (Butterworth and Company, London, 1961).

5. Williams, R. W., Accuracy of Bubble Location in a Bubble Chamber, Rev. Sci. Instr. 32, 1378 (1961).

6. Seitz, F., On the Theory of the Bubble Chamber, Phys. Fluids 1, 2 (1958).

7. Glasstone, S., Sourcebook on Atomic Energy (D. Van Nostrand Company, Inc., Princeton, New Jersey, 1958) p. 160.

8. Blumenfeld, H. A., Bowen, T., and McIlwain, R. L., A 5-Liter Rapid-Cycling Propane or Freon Bubble Chamber; and Blumenfeld, H. A., Bowen, T., McIlwain, R. L., Scheibner, M., Seidlitz, L., Sun, C. R., Design of a 30-Liter Rapid-Cycling Hydrogen Bubble Chamber with Counter-Controlled Photography. Both in Proceedings of an International Conference on Instrumentation for High-Energy Physics, Berkeley, 1960 (Interscience Publishers, Inc., New York, 1961).

9. Glaser, D. A., Progress Report on the Development of Bubble Chambers, Nuovo Cimento Suppl. 11, 361 (1954).

10. Glaser, D. A., Some Effects of Ionizing Radiation on the Formation of Bubbles in Liquids, Phys. Rev. 87, 665 (1952).

11. Parmentier, D., and Schwemin, A., Liquid Hydrogen Bubble Chamber, University of California Radiation Laboratory Report UCRL-2923, March 1955 (unpublished) p. 954.

12. Dittler, H. C., and Gerecke, T. F. Liquid Hydrogen Bubble Chamber, University of California Radiation Laboratory Report UCRL-2985, May 1955 (unpublished).

13. Gow, J. D., Development and Operation of Liquid Hydrogen Bubble Chambers, UCRL-8081, April 1958 (unpublished).

14. Blumberg, R. L., Gow, J. D., and Schwemin, A. J., The Development and Operation of the 10-inch Liquid Hydrogen Bubble Chamber, in Advances in Cryogenic Engineering (Plenum Press, New York, 1960), Vol. 2.

15. Slatis, H., On Bubble Chambers, Nucl. Instr. Methods 5, 1 (1959).

16. Butler, C. C., Britain's National Hydrogen Bubble Chamber, The New Scientist, January 7, 1960, p. 22.

17. Riddiford, L., et al., Some Features of the British National Hydrogen Bubble Chamber, in Proceedings of the International Conference on High-Energy Accelerators and Instrumentation, CERN, 1959 (CERN, Geneva, 1959).

18. Peyrou, C., Some Features of CERN Hydrogen Bubble Chambers, in Proceedings of the International Conference on High-Energy Accelerators and Instrumentation, CERN, 1959 (CERN, Geneva, 1959).

19. Rahm, D. C., Discussion on Brookhaven 20-inch and 80-inch Hydrogen Chambers, in Proceedings of the International Conference on High-Energy Accelerators and Instrumentation, CERN, 1959 (CERN, Geneva, 1959).

20. Hahn, B., Riepe G., and Knudsen, A. W., Some Liquids for Use in Large Bubble Chambers, Rev. Sci. Instr. 30, 654 (1959).

21. Friedman, A., The Thermodynamic and Transport Properties of Liquid Hydrogen and Its Isotopes, National Bureau of Standards Report No. 3282, May 1, 1954 (unpublished).

22. Myall, J., Determination of Bulk Modulus and Sonic Velocity in Superheated Liquid Hydrogen and Superheated Liquid Deuterium, Lawrence Radiation Laboratory Report UCID-1234 Rev. 1, Jan. 1961 (unpublished).

23. Drayer, D. E., and Flynn, T. N., A Compilation of the Physical Equilibria and Related Properties of the Hydrogen-Helium System, National Bureau of Standards Technical Note 109, June 1961 (unpublished).

24. Gow, J. D., and Rosenfeld, A. H., Berkeley 72-Inch Hydrogen Bubble Chamber, in Proceedings of the International Conference on High Energy Accelerators and Instrumentation CERN, 1959 (CERN, Geneva, 1959).

25. Hernandez, H. P., Cryogenic Experiences with the 72-Inch Bubble Chamber, in Advances in Cryogenic Engineering, (Plenum Press, New York, 1960) Vol. 5.

26. Lucas, L. R., 72-Inch Bubble Chamber, Stainless Steel Selection, University of California Radiation Laboratory Report UCID-85, April 1957 (unpublished).

27. Goodzeit, C., Evaluation of Stainless Steel Casting Alloys for the 80-Inch Chamber Body and Associated Parts, Brookhaven National Laboratory Report E-95, BC-01-1G, July 1961 (unpublished).

28. Schaeffler, A. L., Welding Dissimilar Metals with Stainless Electrodes, Iron Age 162, No. 1, 72 (1948).

29. Eichelman, G. H., and Hull, F. C., The Effect of Composition on the Temperature of Spontaneous Transformation of Austenite to Martensite in 18-8 Type Stainless Steel, in Proceedings of the 34th National Metal Congress and Exposition, Philadelphia, October 1952 (American Society for Metals, Cleveland, Ohio, 1953).

30. Kropschot, R. H., and Mikeseli, R. P., An Experimental Study of the Strength and Fatigue of Glass at Very Low Temperatures, National Bureau of Standards Report 3590, Technical Memorandum No. 37, June 1956 (unpublished).

31. Lucas, L., 72-Inch Bubble Chamber, Glass Cool Down Summary, University of California Radiation Laboratory Report UCID-219, September 1957 (unpublished).

32. Franck, J., Optical Windows and Seals for Hydrogen Bubble Chambers, University of California Radiation Laboratory Report UCID-71, March 1956 (unpublished).

33. Lucas, L., and Hernandez, H. P., Inflatable Gasket for the 72-Inch Bubble Chamber, Rev. Sci. Instr. 30, 941 (1959).

34. Hernandez, H. P., The 72-Inch Bubble Chamber: Report of the First Liquid Nitrogen Run, University of California Radiation Laboratory Report UCID-483, October 1958 (unpublished).

35. Hart, J., Tanforan, F., and Lucas, L., 72-Inch Chamber Hydrostatic Test, University of California Radiation Laboratory Report UCID-549, March 1958 (unpublished).

36. Tanforan, F., and Smits, R., 72-Inch Chamber Hydraulic Jack Test, University of California Radiation Laboratory Report UCID-553, July 1958 (unpublished).

37. Lucas, L., 72-Inch Chamber, Glass Pre-Load Setting, University of California Radiation Laboratory Report UCID-348, August 1958 (unpublished).

38. Hitchcock, H. C., and Watt, R. D., Reduction of Optical Distortion in Gas-Expansion Bubble Chambers, in Proceedings of an International Conference on Instrumentation for High-Energy Physics, Berkeley, 1960 (Interscience Publishers, Inc., New York, 1961).

39. Barrera, F., 72-Inch Bubble Chamber Expansion System, Lawrence Radiation Laboratory Report UCID-737, March 1959 (unpublished).

40. Norgren, D., 25-Inch Bubble Chamber Optics Distorting; Its Effect on Film Centering Tolerances, Lawrence Radiation Laboratory Report UCID-1678, April 1962 (unpublished).

41. Barford, N. C., Low-Temperature Bubble Chambers, in Progress in Cryogenics (Academic Press, Inc., New York, 1960), Vol. 2, p. 87.

42. Chelton, D. B., Mann, D. B., and Birmingham, B. W., An Intermediate Size Automatically Controlled Hydrogen Refrigeration System, International Institute of Refrigeration, Proceedings Commission I, Eindhoven, 1960.

43. Chelton, D. B., Dean, J. W., and Birmingham, B. W., Closed Circuit Hydrogen Refrigeration System, Rev. Sci. Instr. 31, 712 (1960).

44. Schmeissner, F., and Hänny, J., Refrigeration Plant for the Two-metre Hydrogen Bubble Chamber of the European Organization for Nuclear Research (CERN), Sulzer Technical Review No. 3, 1961 (unpublished).

45. Hernandez, H. P., Procedures for the Design and Operation of Hazardous Research Equipment, Lawrence Radiation Laboratory Report UCRL-9711, October 1961 (unpublished).

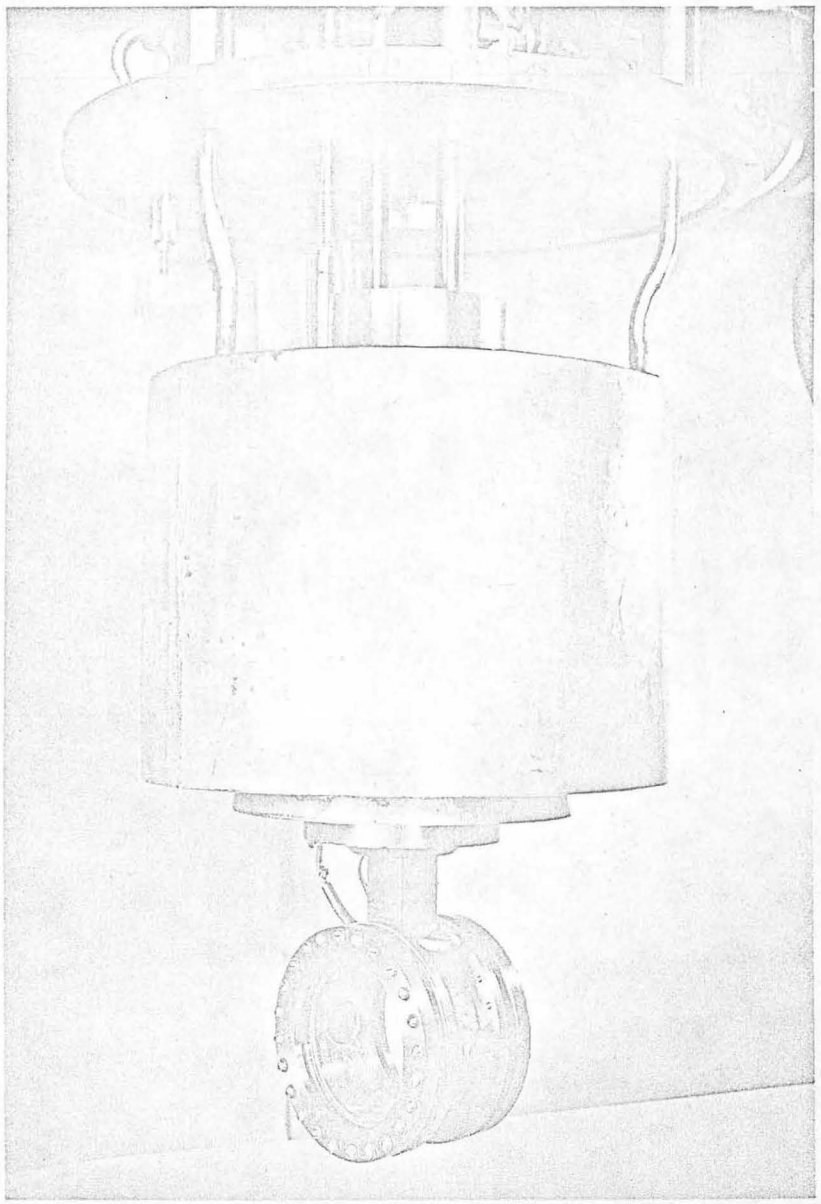

ZN-2100

Fig. 1. The Berkeley 4-inch liquid hydrogen bubble chamber.

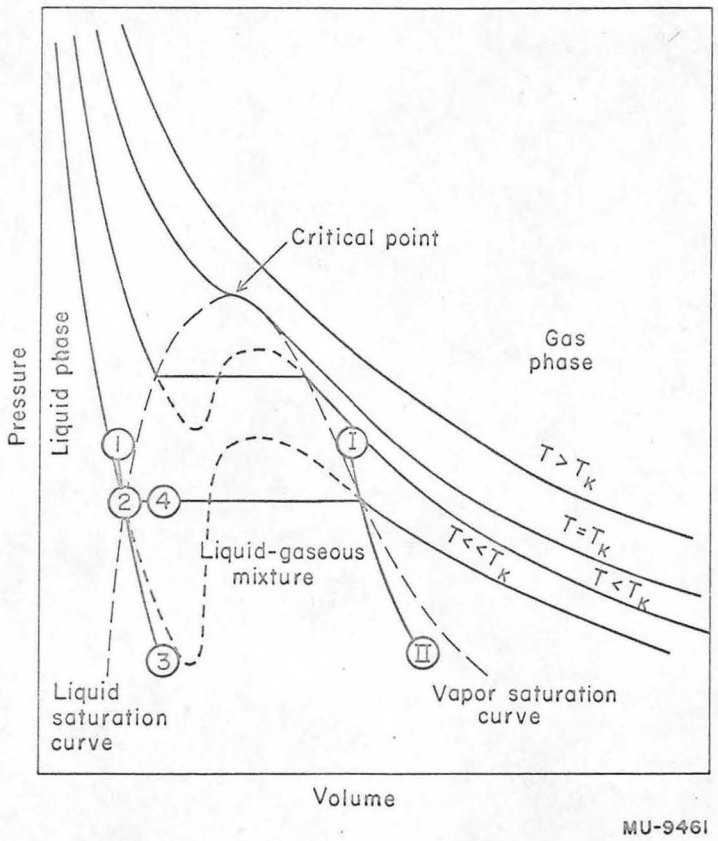

Fig. 2. Pressure-volume plot of representative expansion curves for a real gas, showing zones of operation for bubble chambers ((1) (2) (3) (4)) and cloud chambers ((I) (II)).

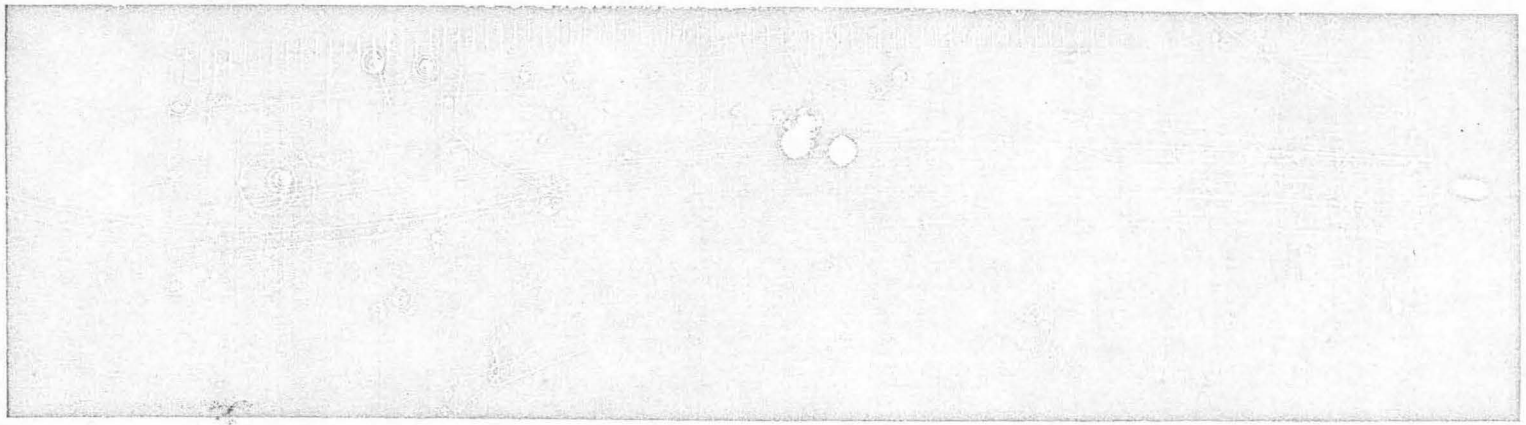

ZN-2484

Fig. 3. Berkeley 72-inch liquid hydrogen bubble chamber track photograph.

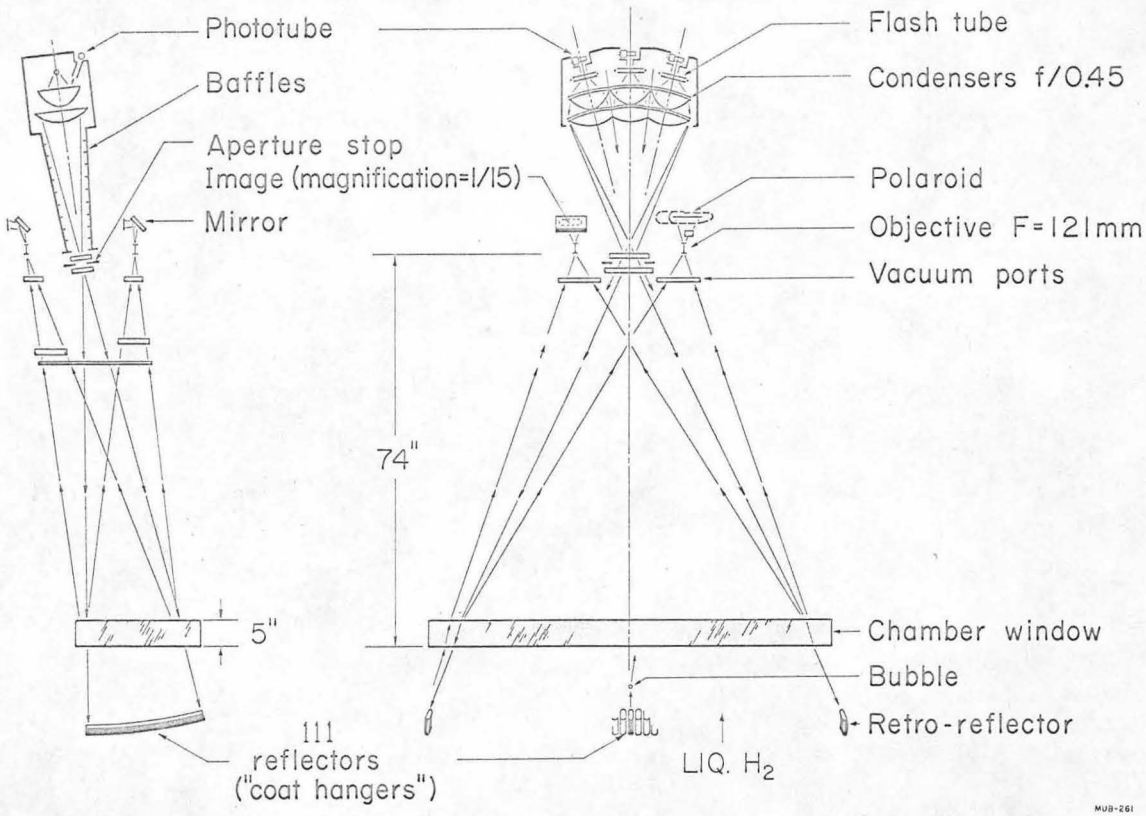

Fig. 4. Optical system of the Berkeley 72-inch bubble chamber.

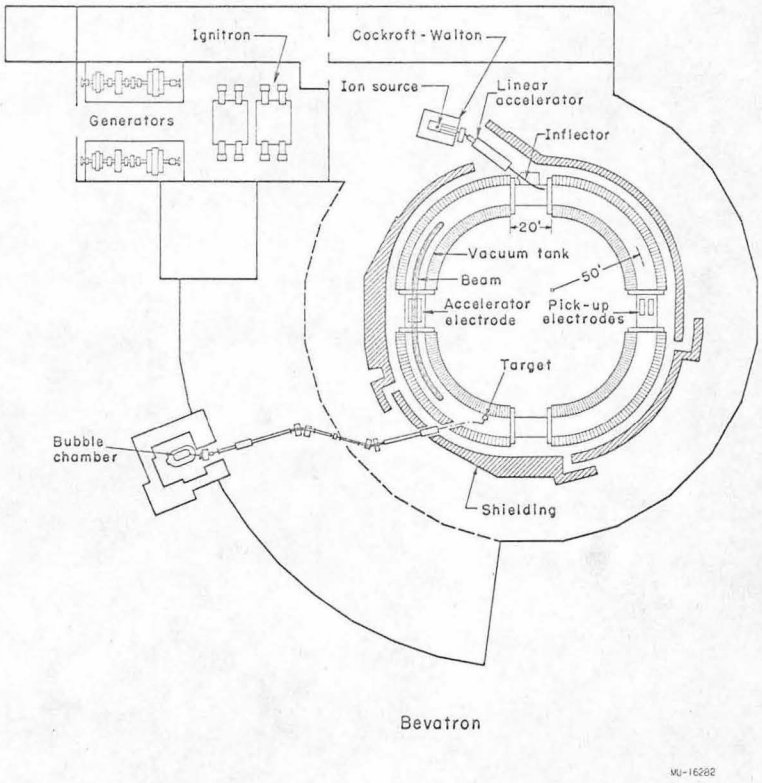

Fig. 5. Particle path from the Bevatron, through the beam path, and into the 72-inch bubble chamber (Berkeley).

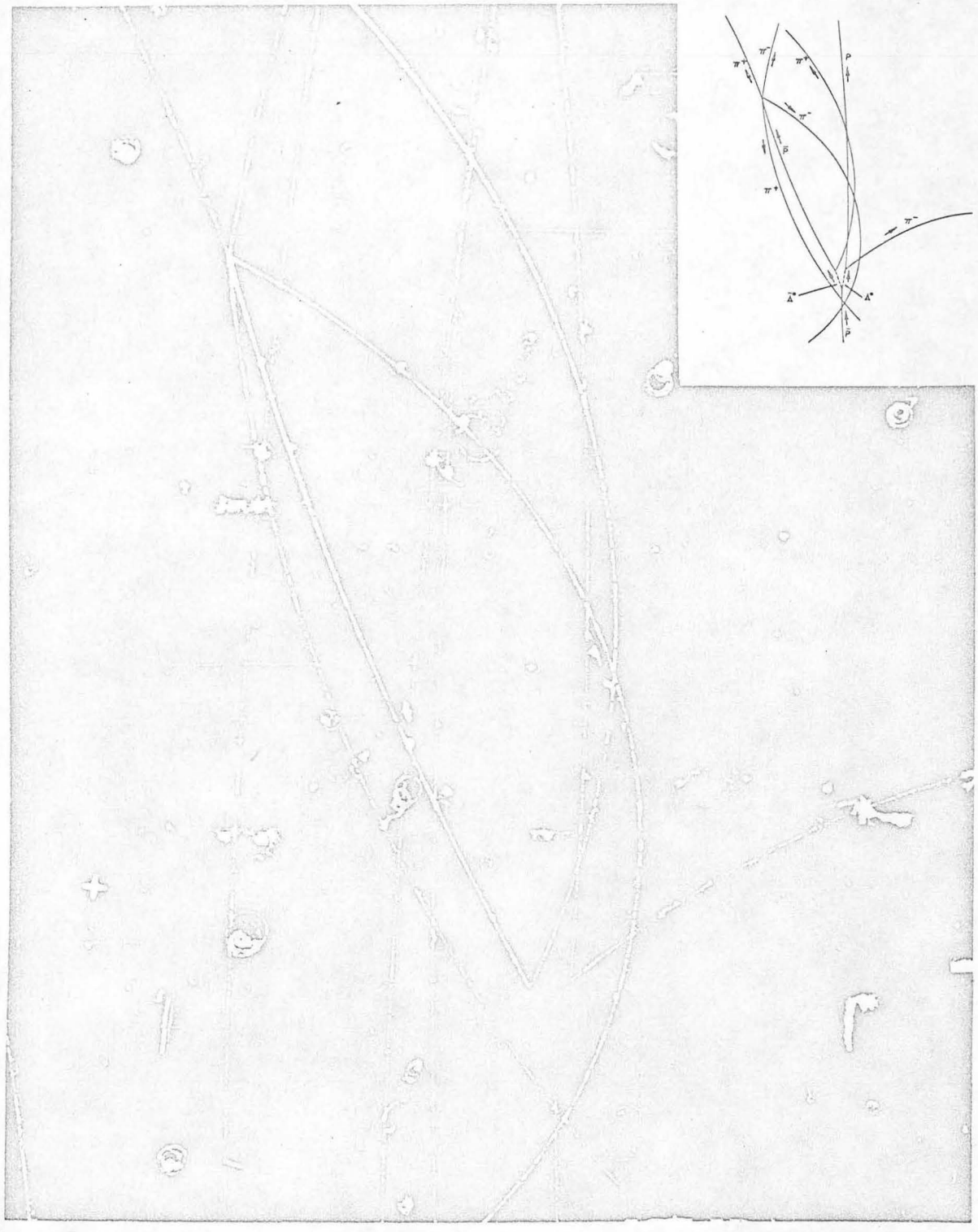

ZN-2485

Fig. 6. Production and decay of neutral lambda and anti-lambda hyperons.

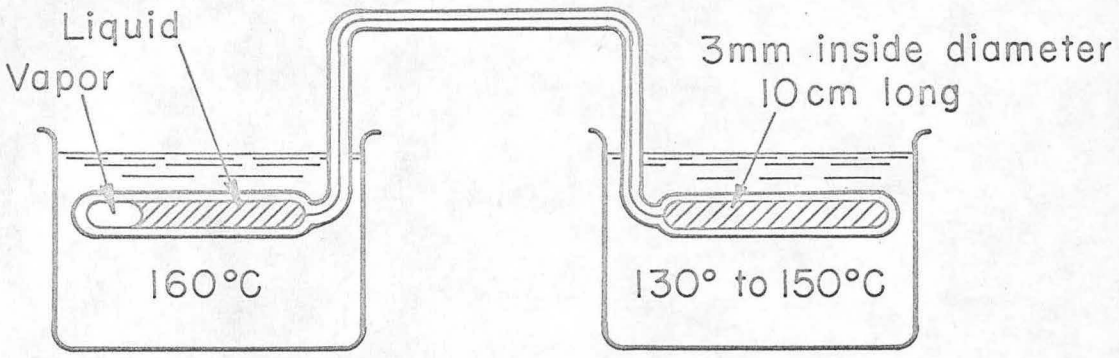

Fig. 7. Glaser's first experiment to demonstrate the radiation sensitivity of superheated diethyl ether (Reference 9).

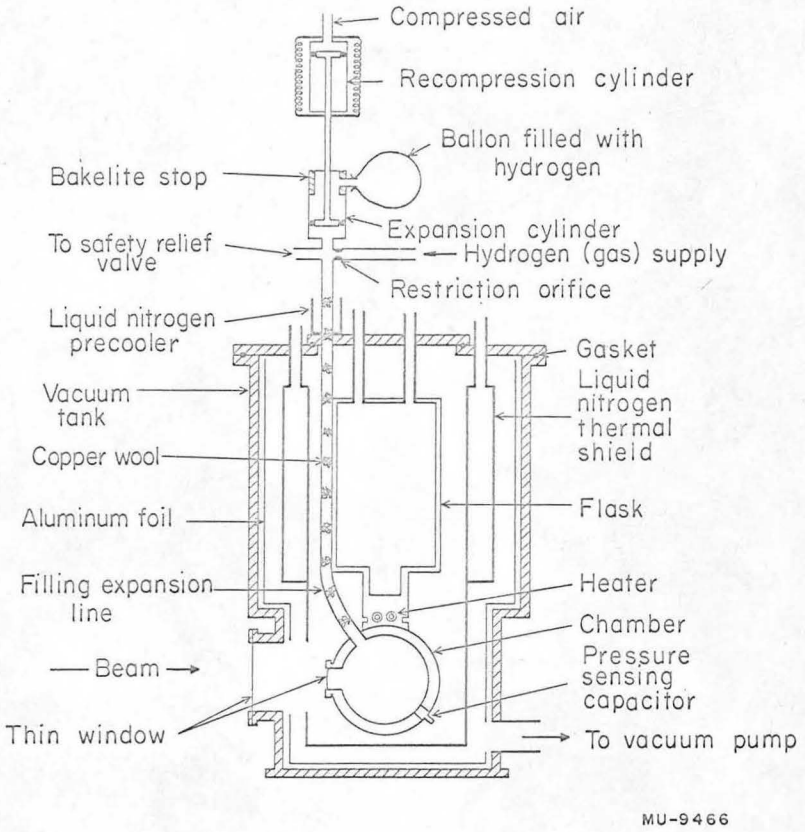

Fig. 8. Cross section of Berkeley 4-inch liquid hydrogen bubble chamber.

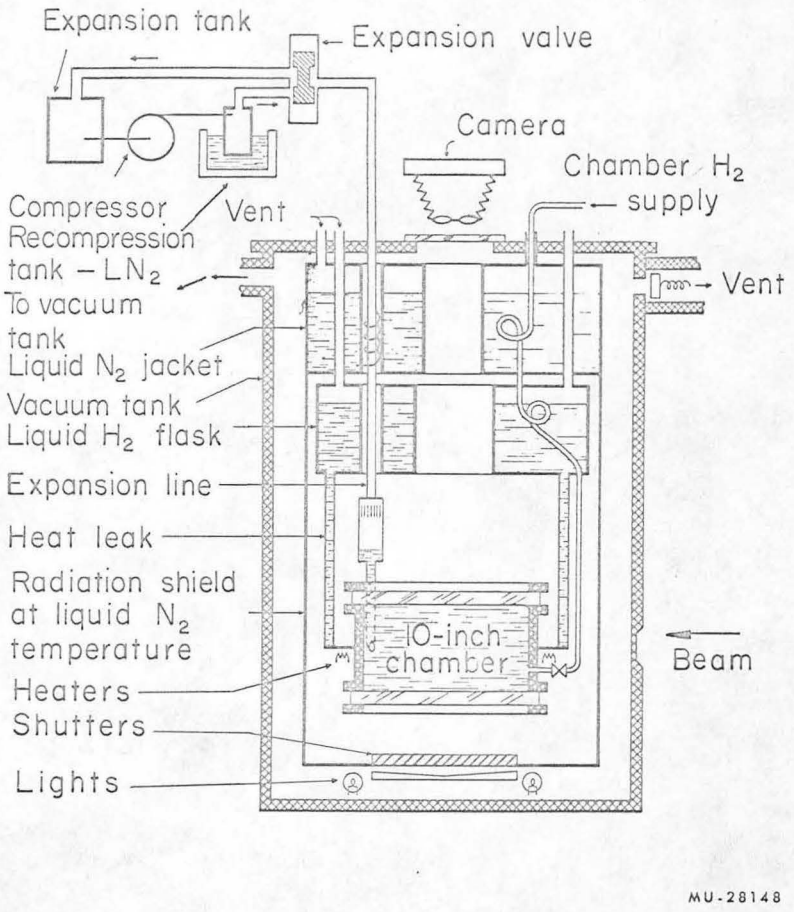

Fig. 9. Berkeley 10-inch liquid hydrogen bubble chamber.

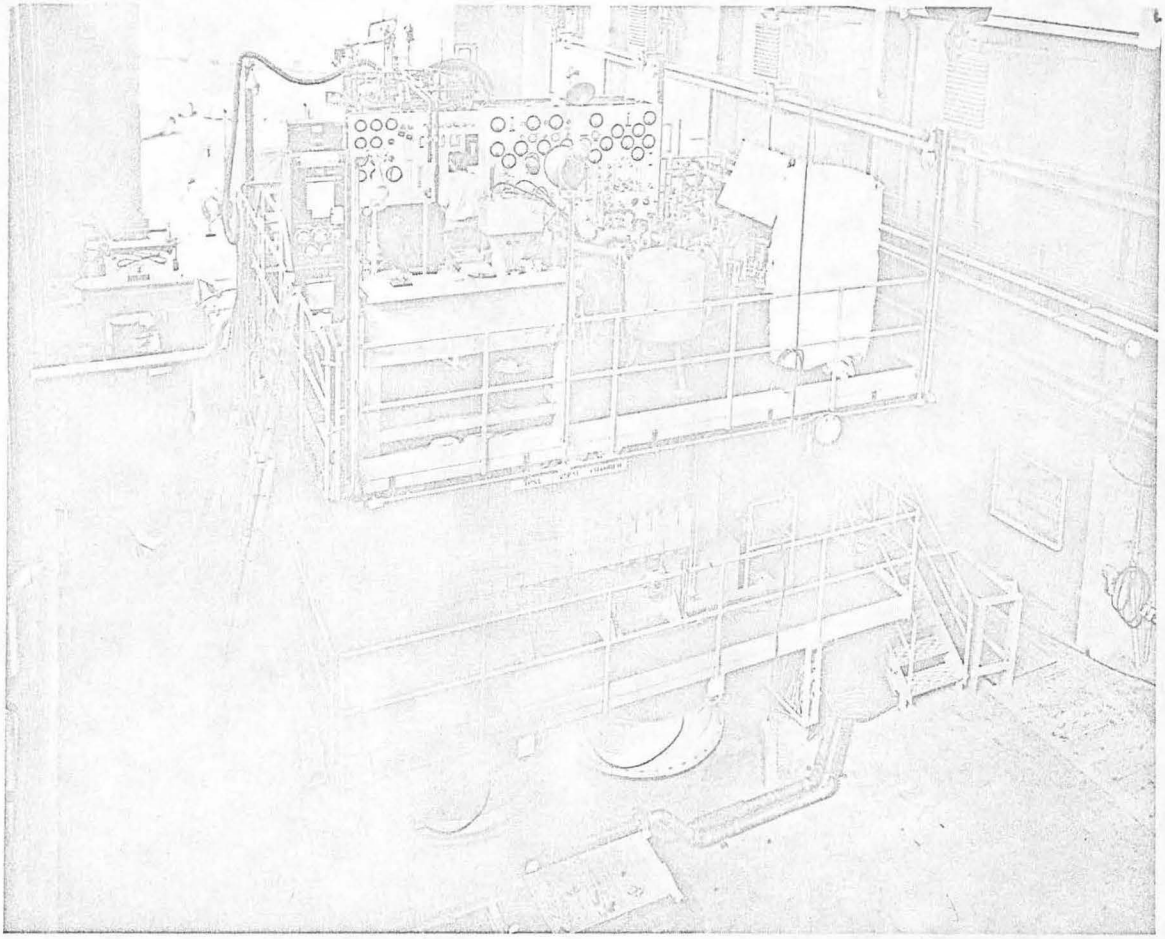

ZN-3299

Fig. 10. Berkeley 72-inch liquid hydrogen bubble chamber.

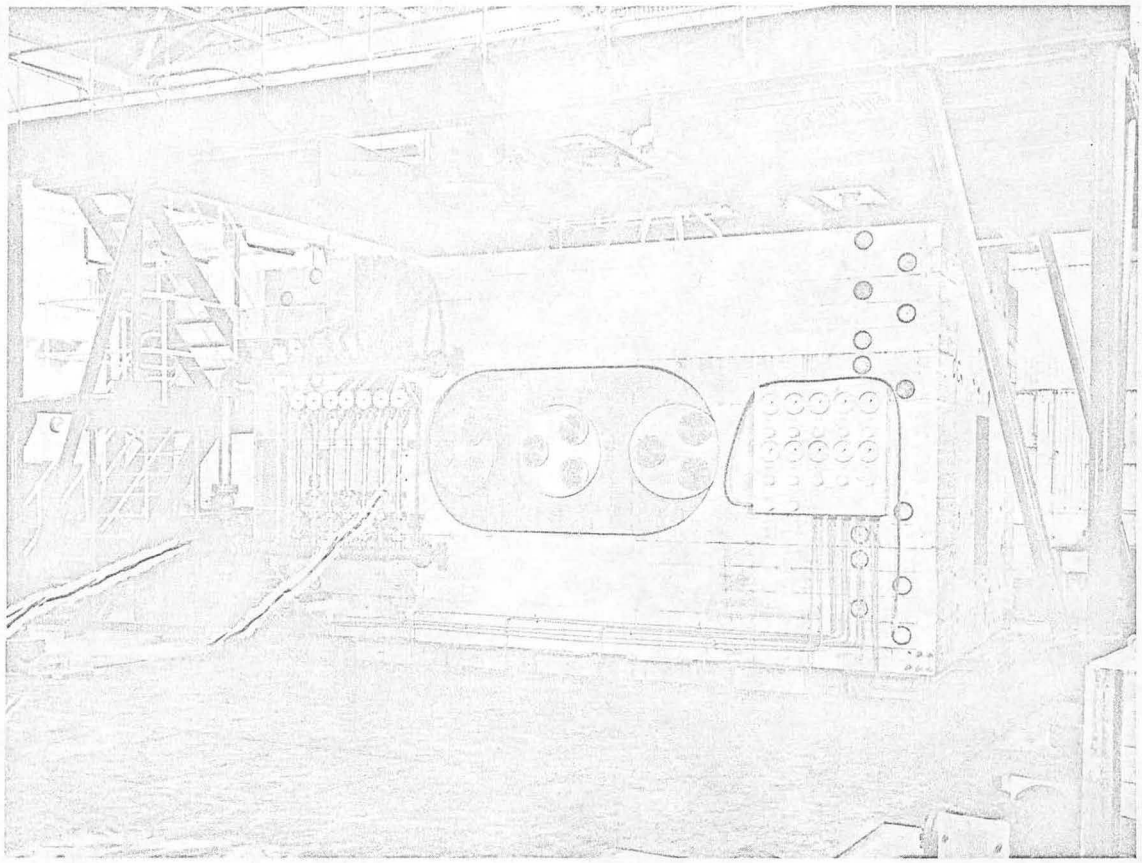

ZN-3297

Fig. 11. The 60-inch British National liquid hydrogen bubble chamber.

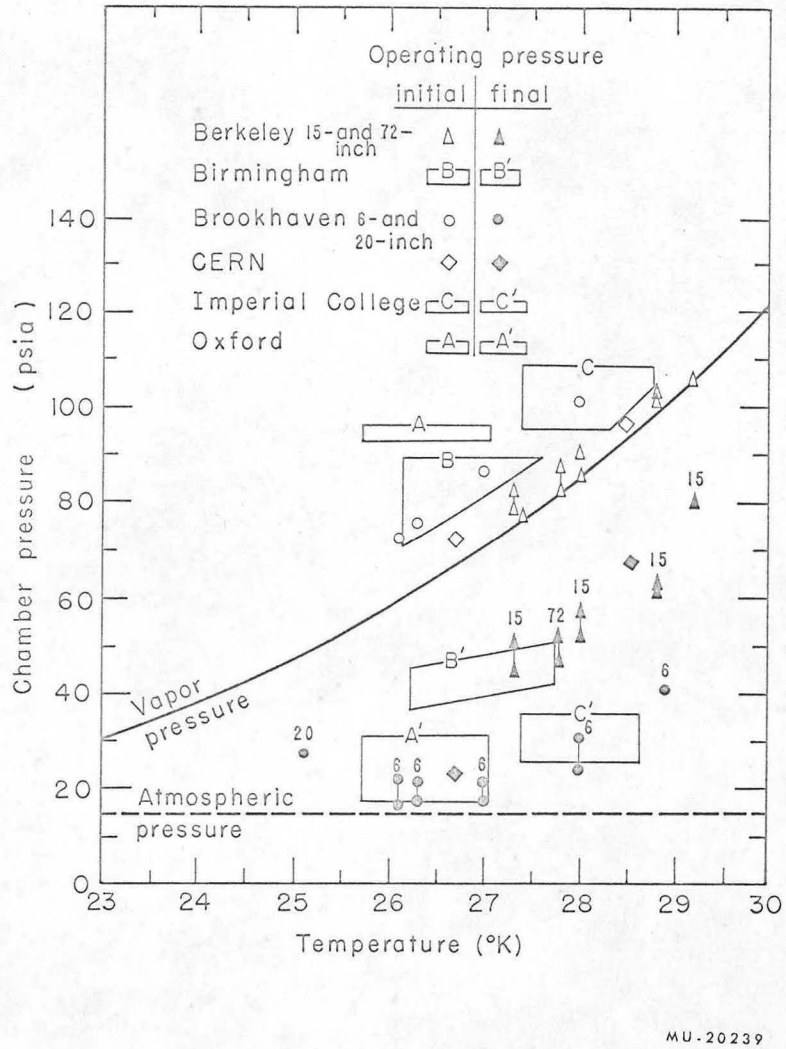

Fig. 12. Normal range of operating temperature and pressure for liquid hydrogen bubble chambers.

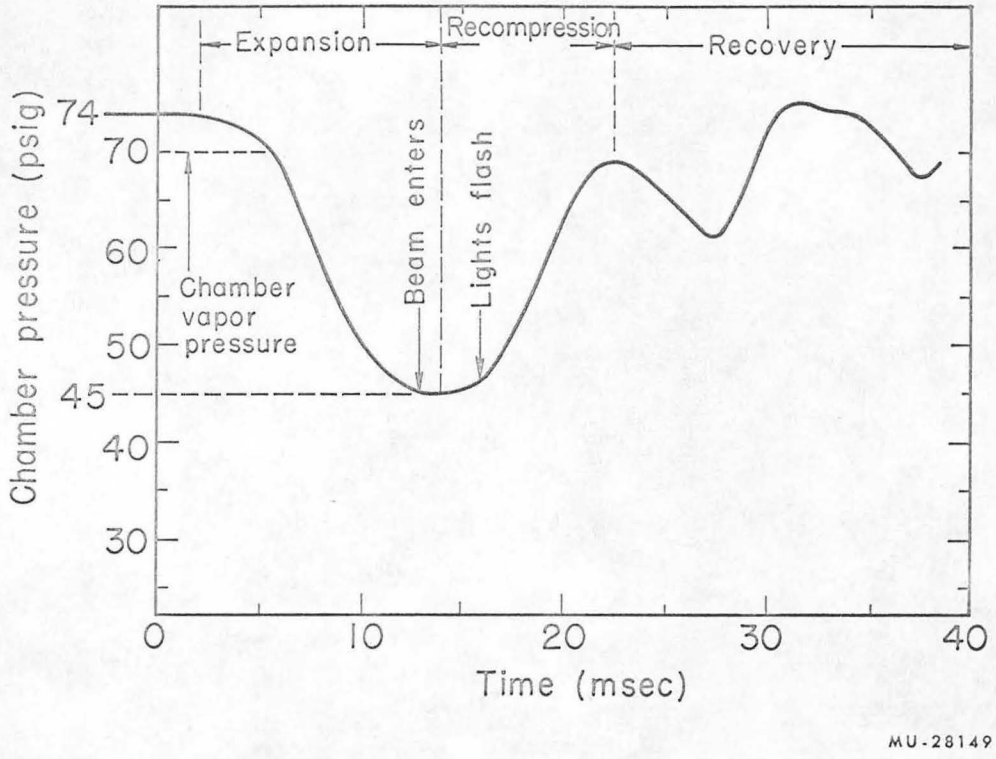

Fig. 13. Typical expansion-recompression cycle for a liquid-hydrogen bubble chamber.

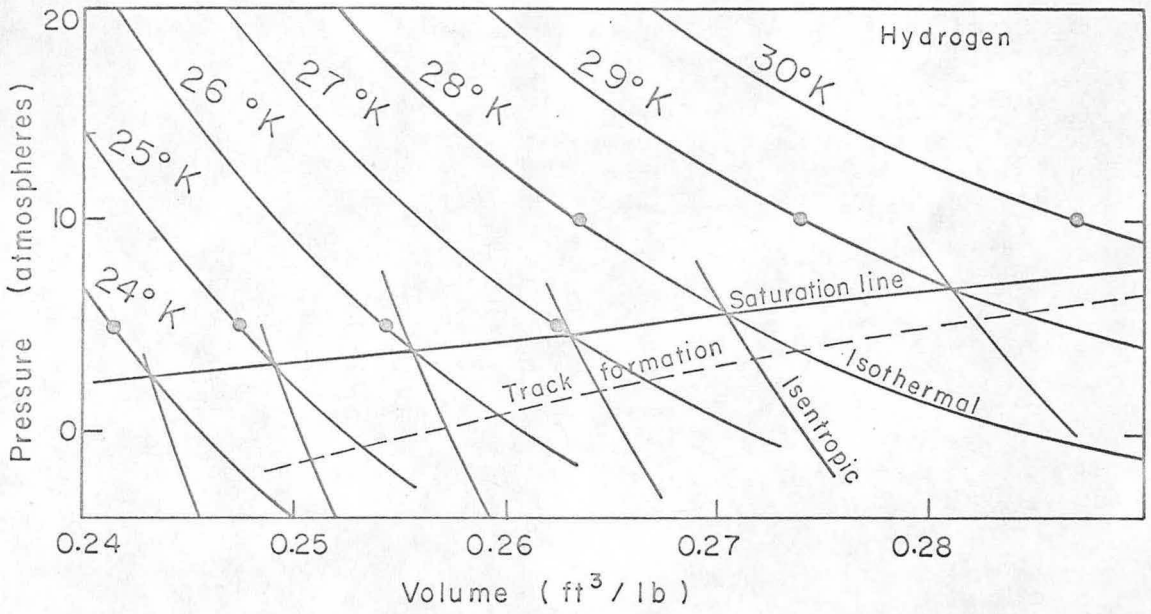

Fig. 14. Isothermal and isentropic pressure-volume curves for hydrogen. These curves were computed below the vapor-pressure line by

$$\left[p + \frac{a}{V^2}\right](V-b) = RT$$

for the isothermal case, and by

$$\left[p + \frac{a}{V^2}\right](V-b)^{\frac{R}{C_V}+1} = \text{constant}$$

for the isentropic case (Reference 22).

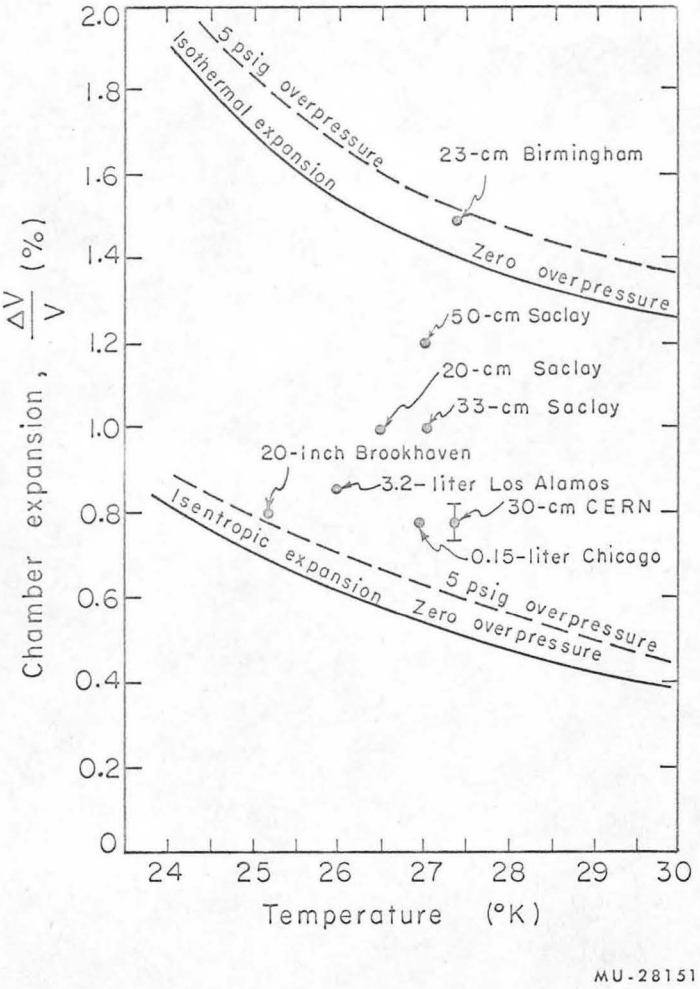

Fig. 15. Change in volume of several liquid hydrogen bubble chambers during the expansion cycle. Chambers with the most efficient expansion systems have lower expansion ratios, $\Delta V/V$, and operate near the isentropic expansion curve.

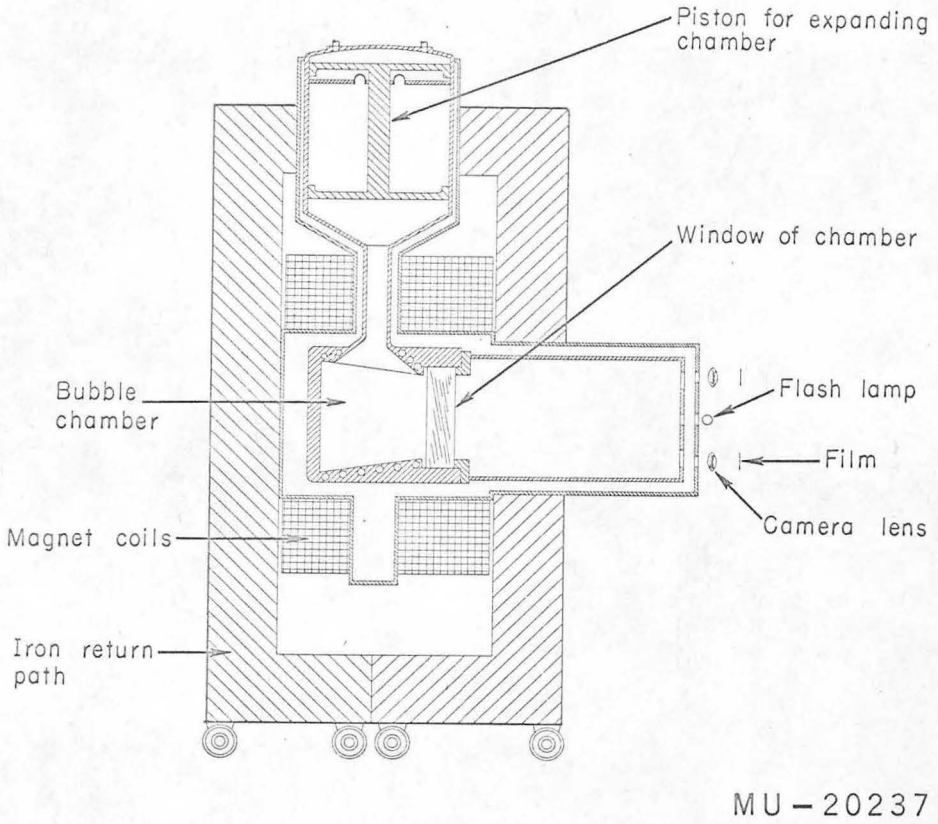

Fig. 16. Transverse cross section of 80-inch Brookhaven liquid hydrogen bubble chamber.

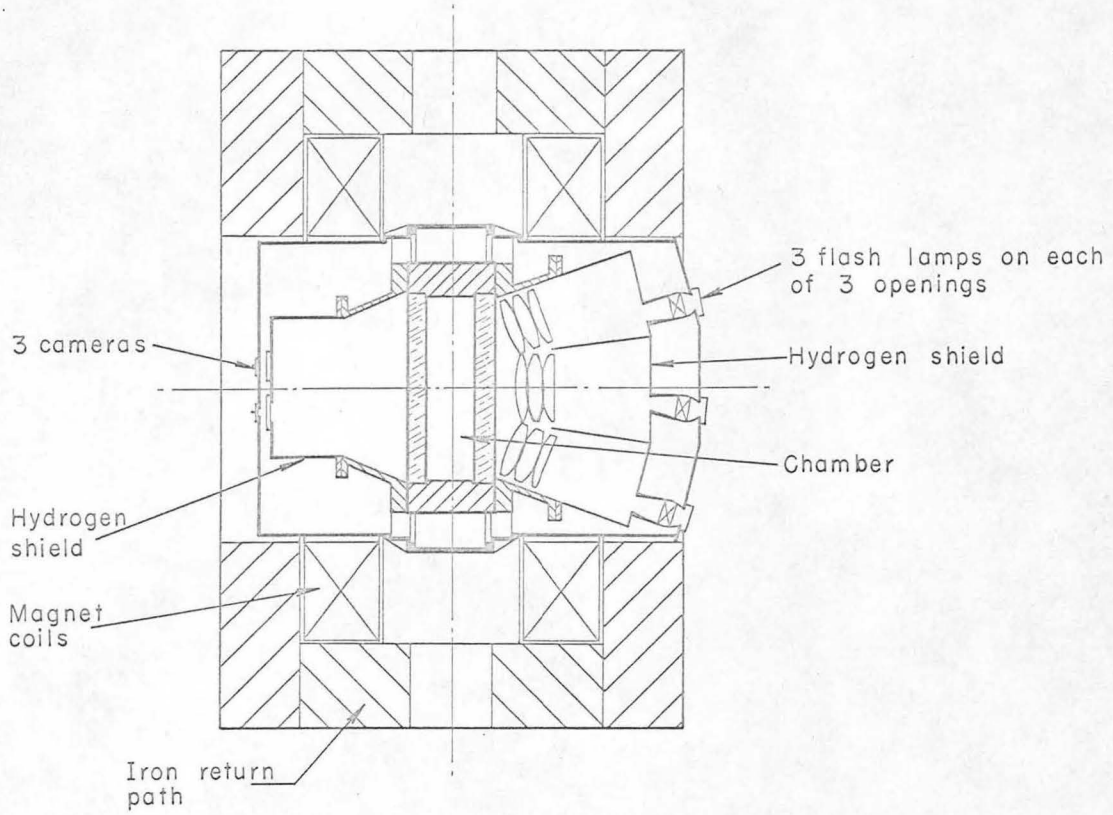

Fig. 17. Plan view of 60-inch British National liquid hydrogen bubble chamber.

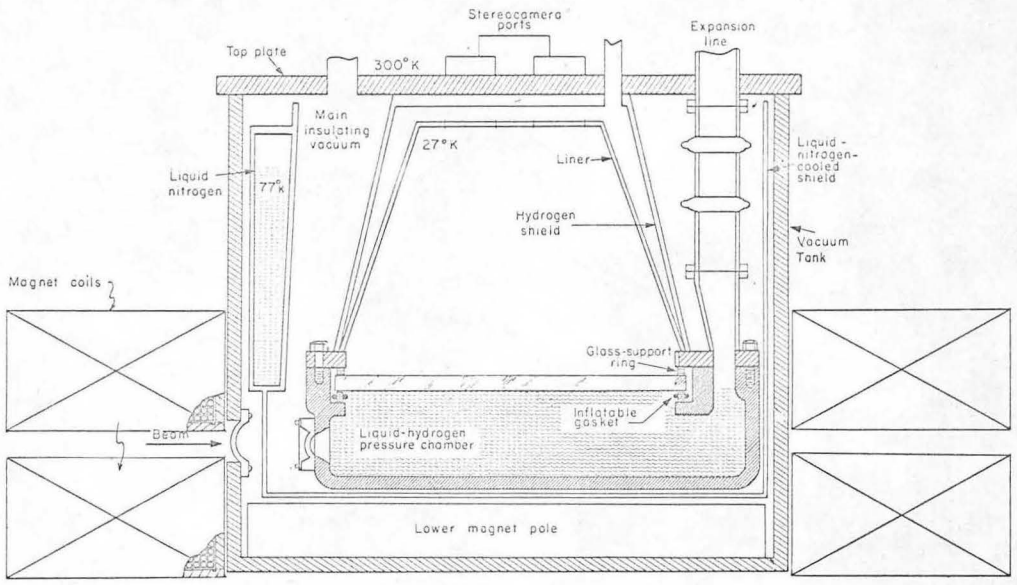

Fig. 18. Longitudinal cross section of the Berkeley 72-inch bubble chamber. (The direction of the magnetic field is vertical.)

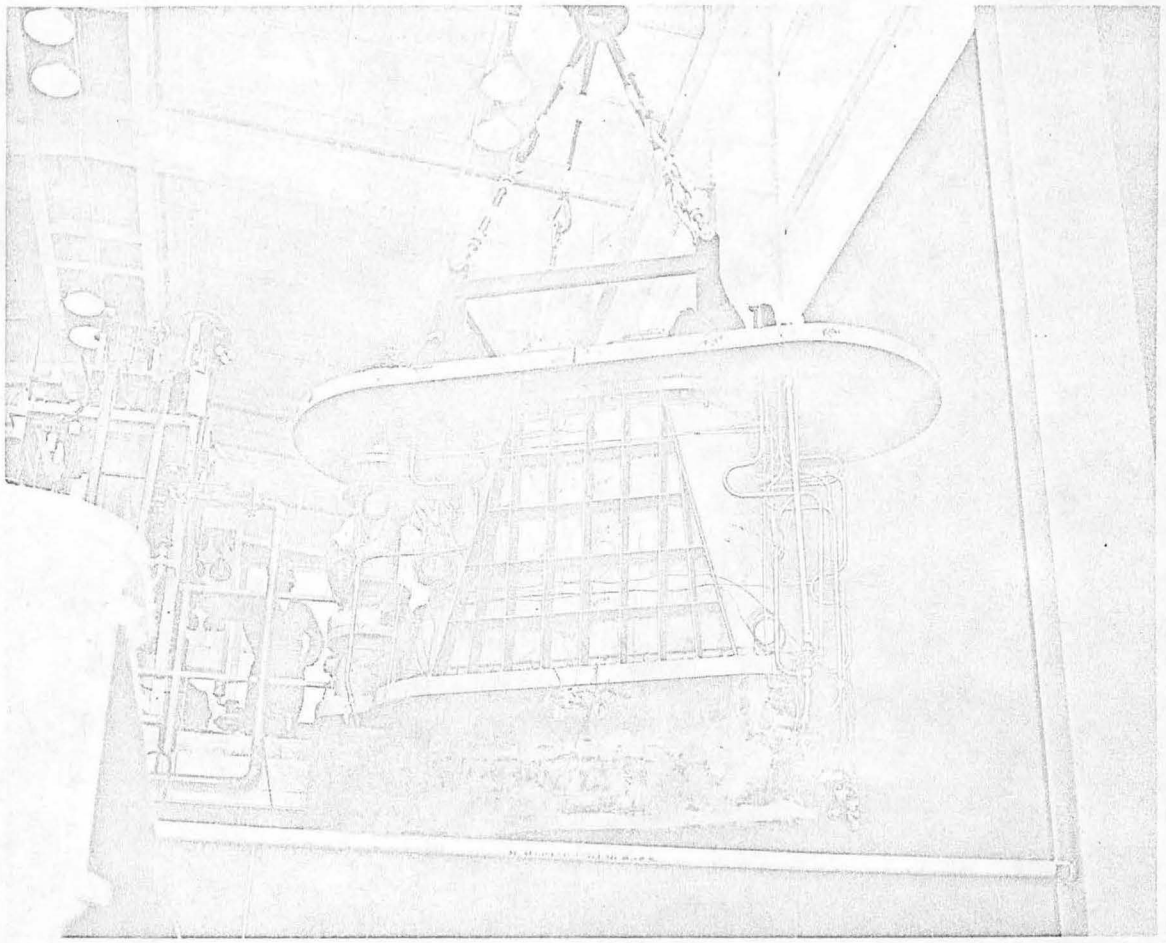

ZN-3300

Fig. 19. Berkeley 72-inch bubble chamber top plate and chamber assembly being installed in the vacuum tank.

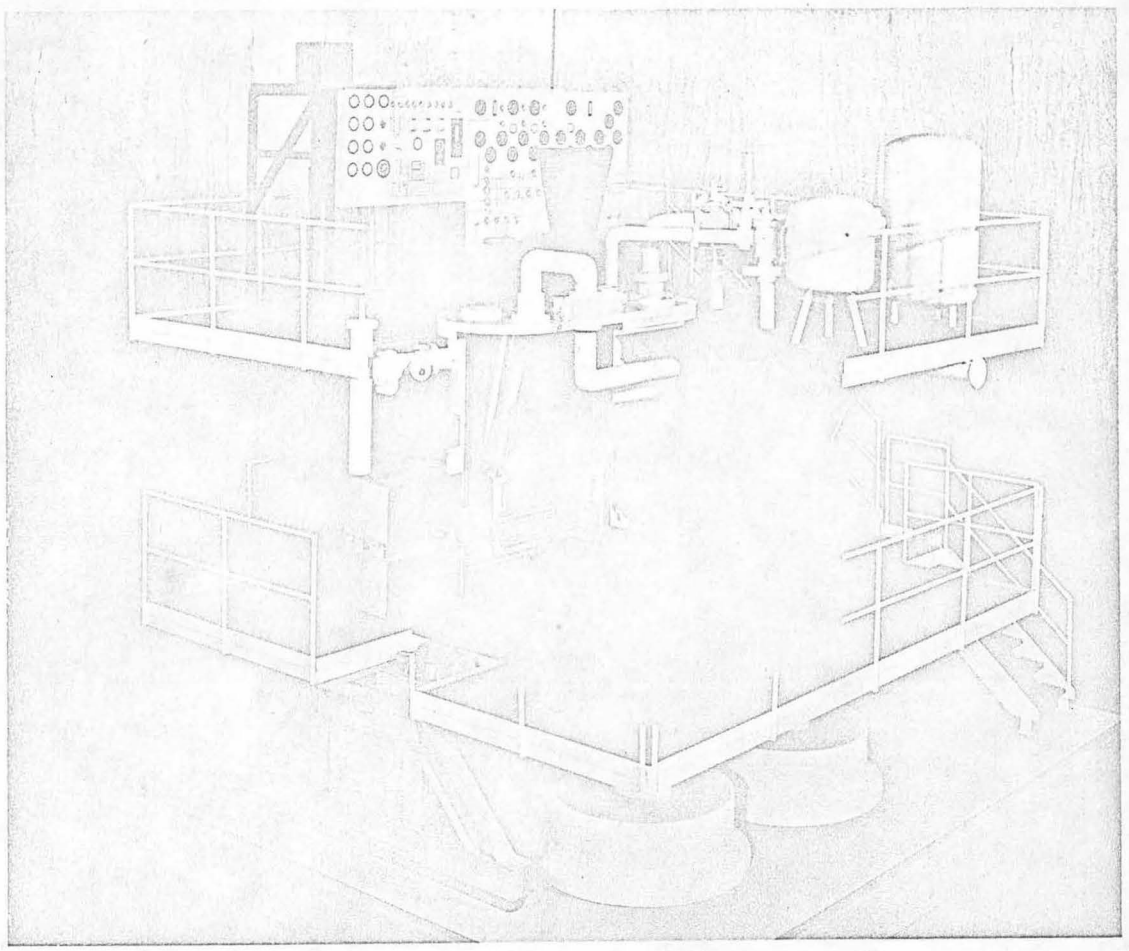

ZN-3304

Fig. 20. Cutaway model of the Berkeley 72-inch bubble chamber.

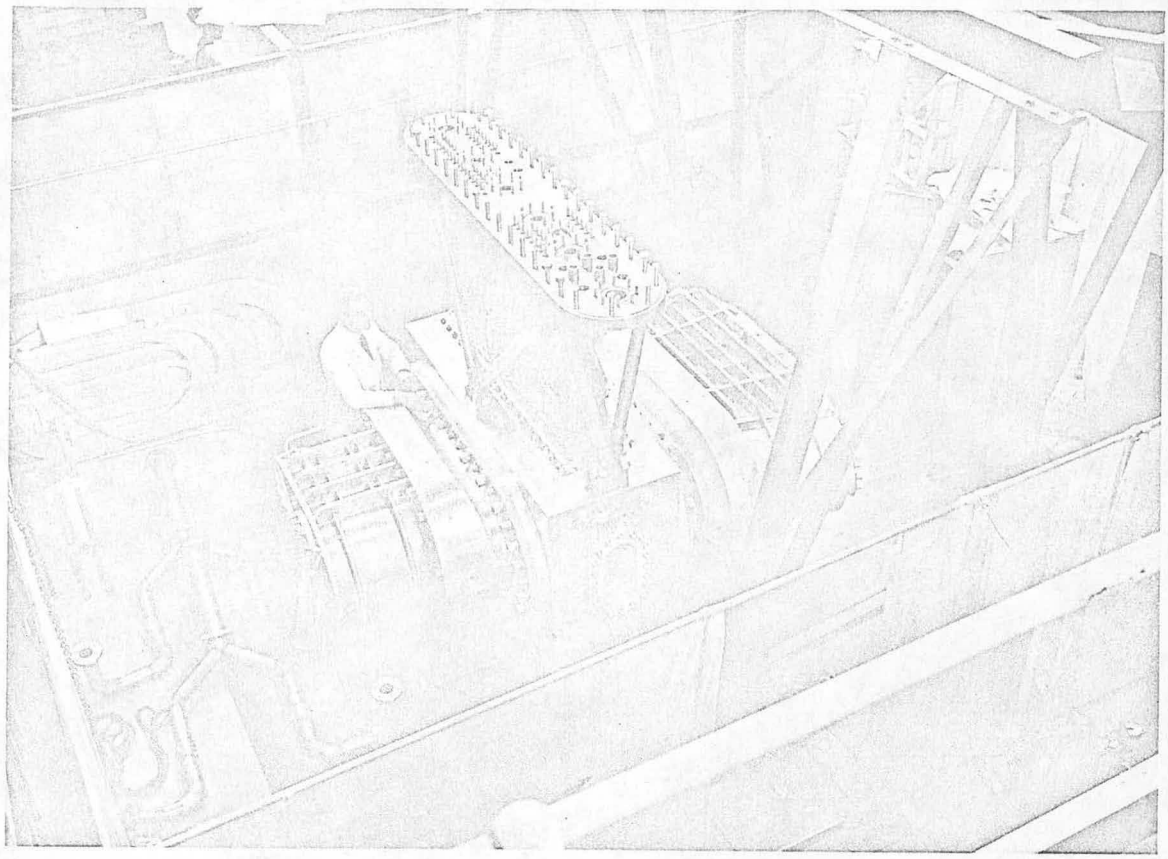

ZN-3298

Fig. 21. Aluminum-alloy chamber body of the 60-inch British National bubble chamber.

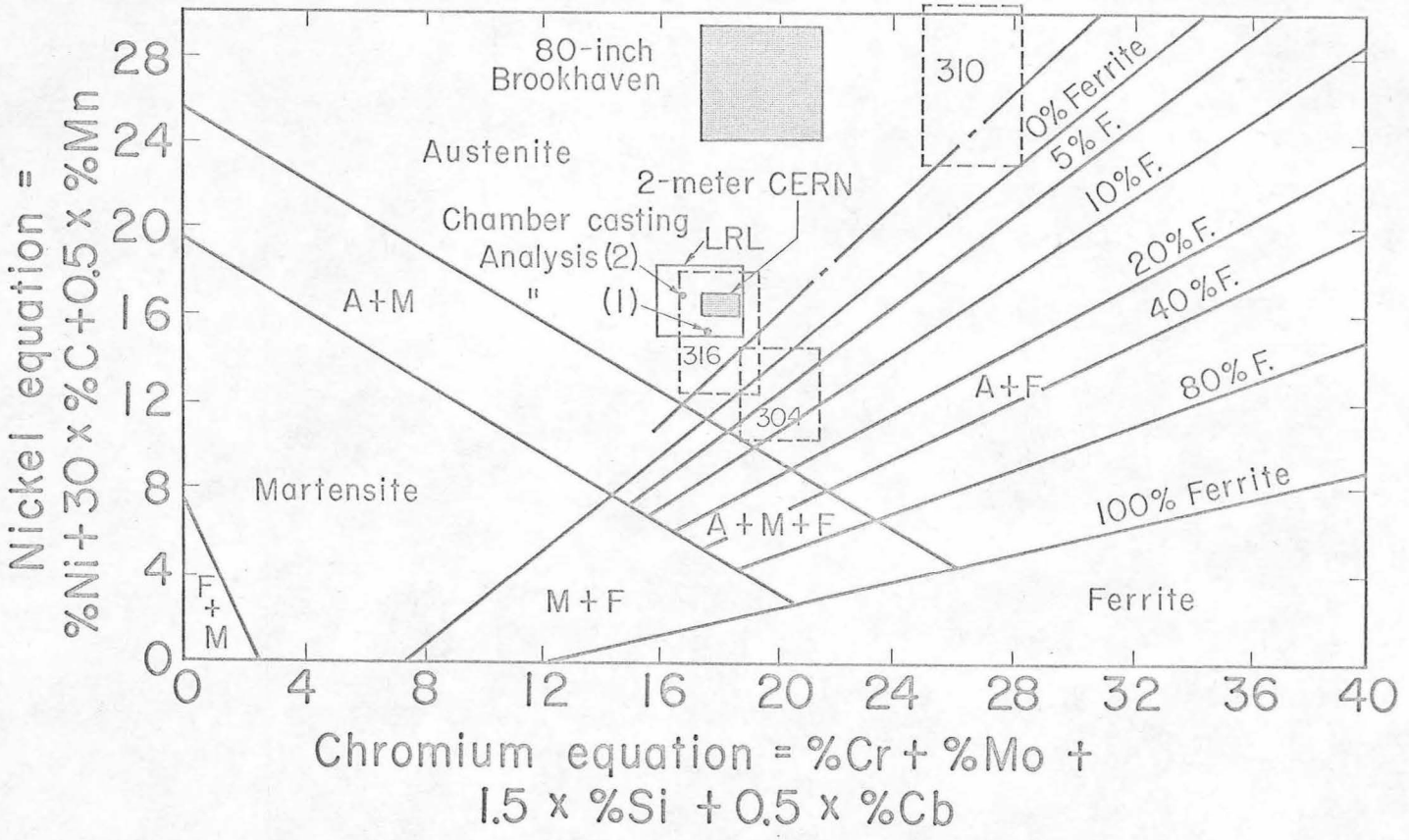

MUB-1342

Fig. 22. Constitution diagram for stainless steel at room temperature. (Courtesy A. L. Schaeffler.)

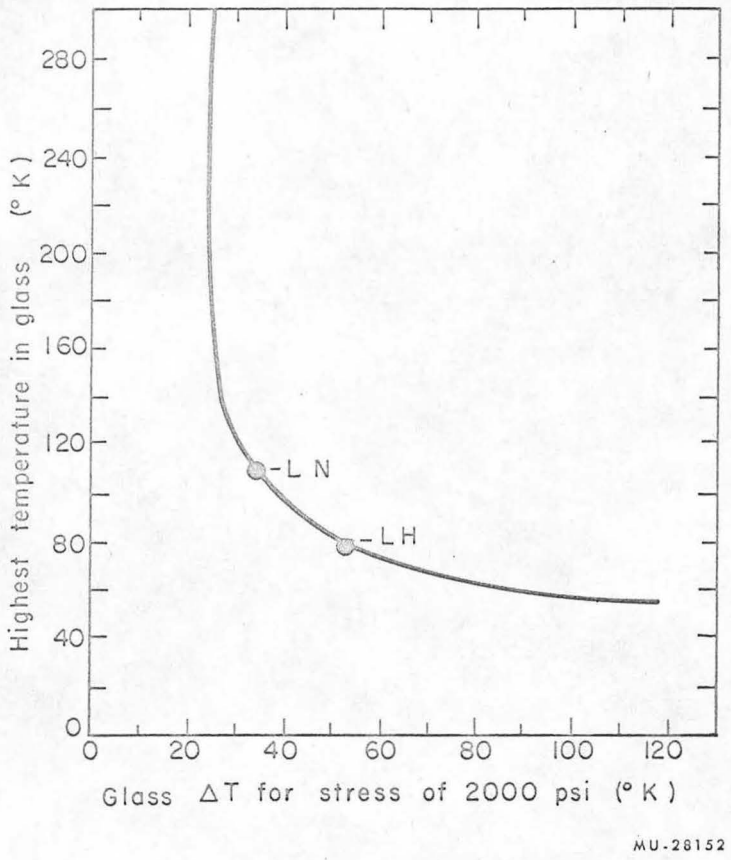

Fig. 23. The allowable temperature difference, ΔT, of the chamber glass to limit the thermal stress to 2000 psi. The points marked LN and LH give the highest temperatures at which LN and LH can make contact with the glass and not stress the glass more than 2000 psi.

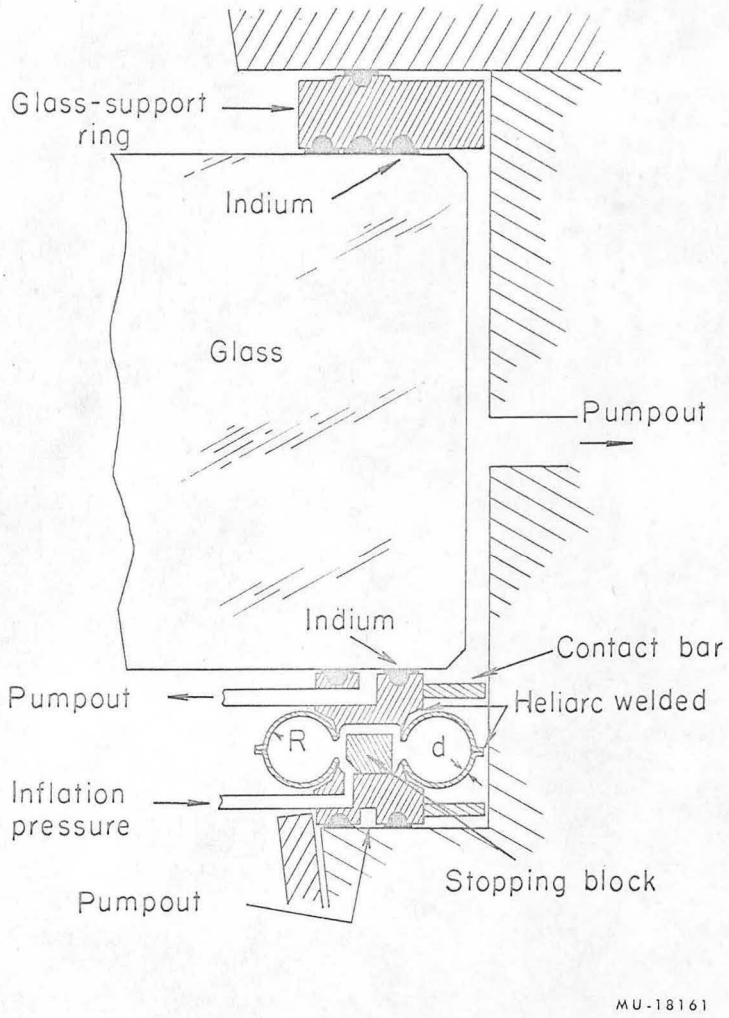

Fig. 24. Cross section of the inflatable gasket and related parts for the Berkeley 72-inch bubble chamber.

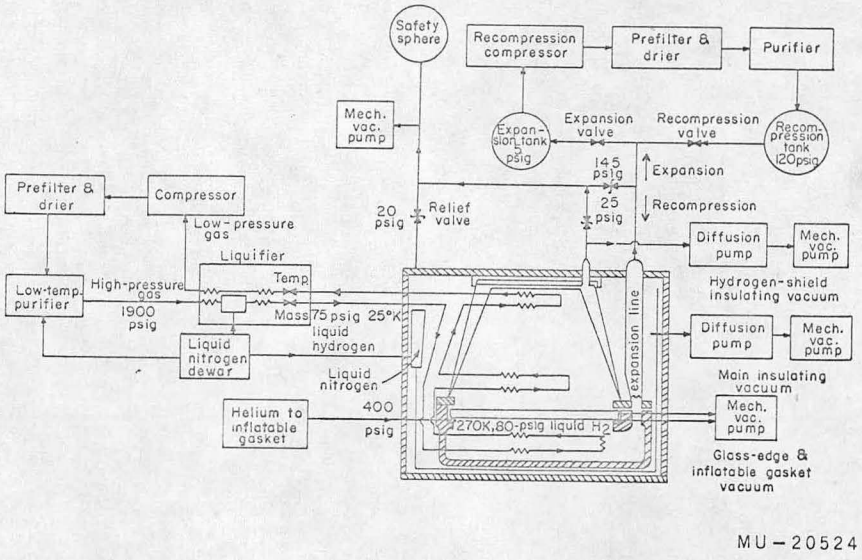

Fig. 25. Simplified schematic of expansion, refrigeration, vacuum, and safety-vent systems for the Berkeley 72-inch bubble chamber.

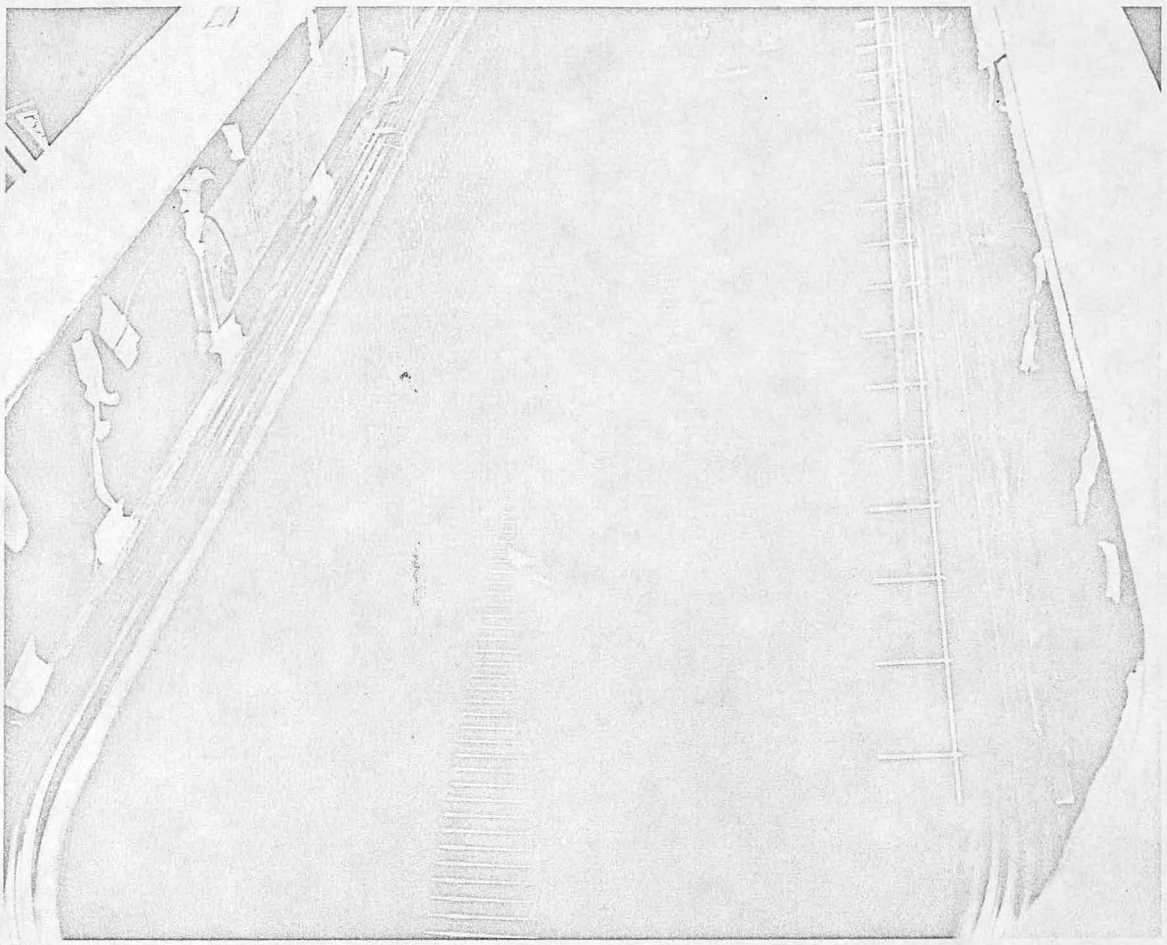

ZN-3301

Fig. 26. Berkeley 72-inch bubble chamber prior to assembly.

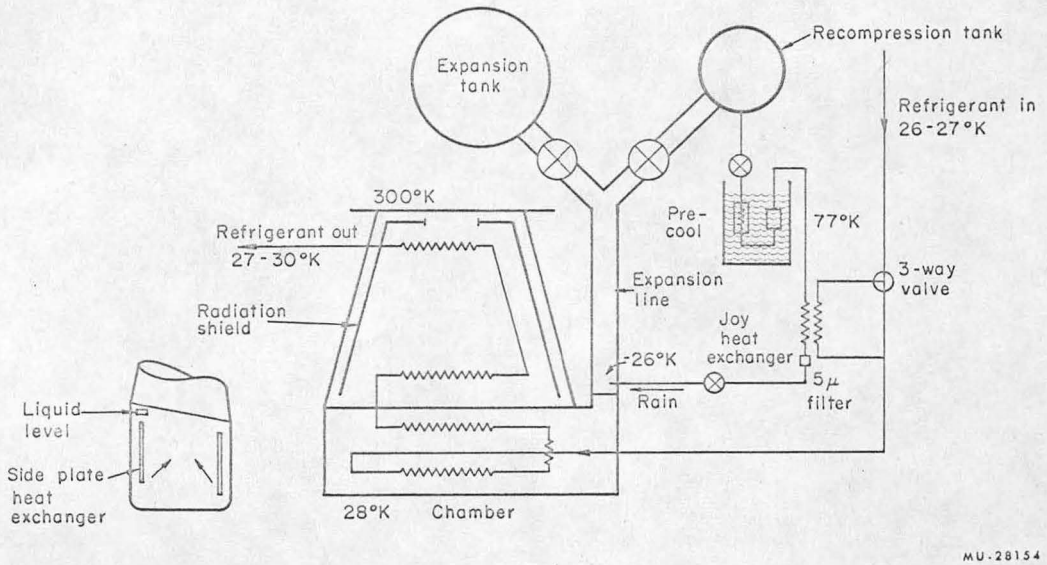

Fig. 27. Schematic representation of refrigeration circuit for the Berkeley 72-inch bubble chamber, showing how liquid hydrogen is introduced into the expansion line at the liquid - gas interface.

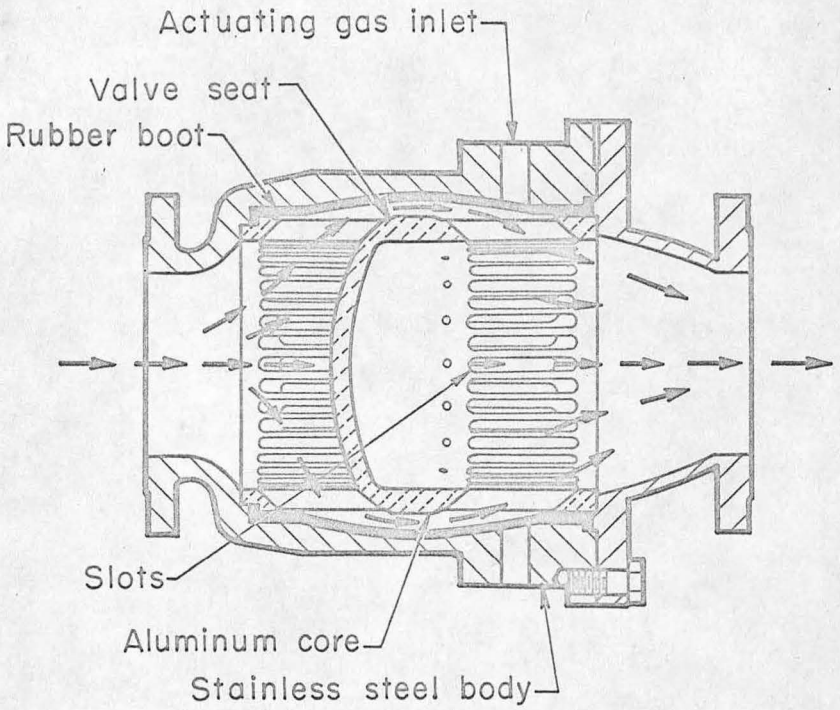

Fig. 28. Grove-type boot valve shown in section.

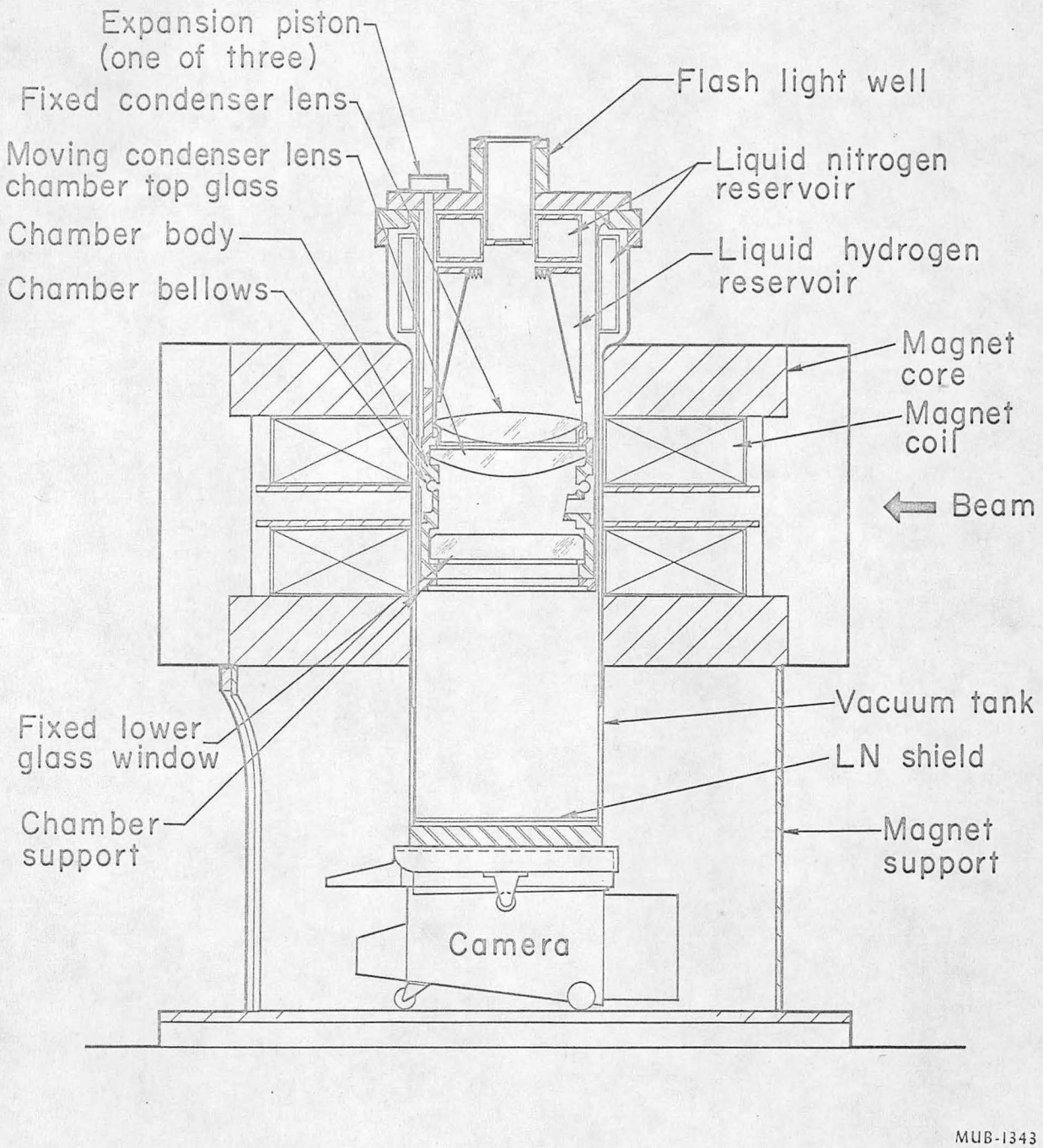

Fig. 29. Cross section of Berkeley 25-inch bubble chamber. (The chamber is divided by a single-convolution bellows that is used to expand the chamber).

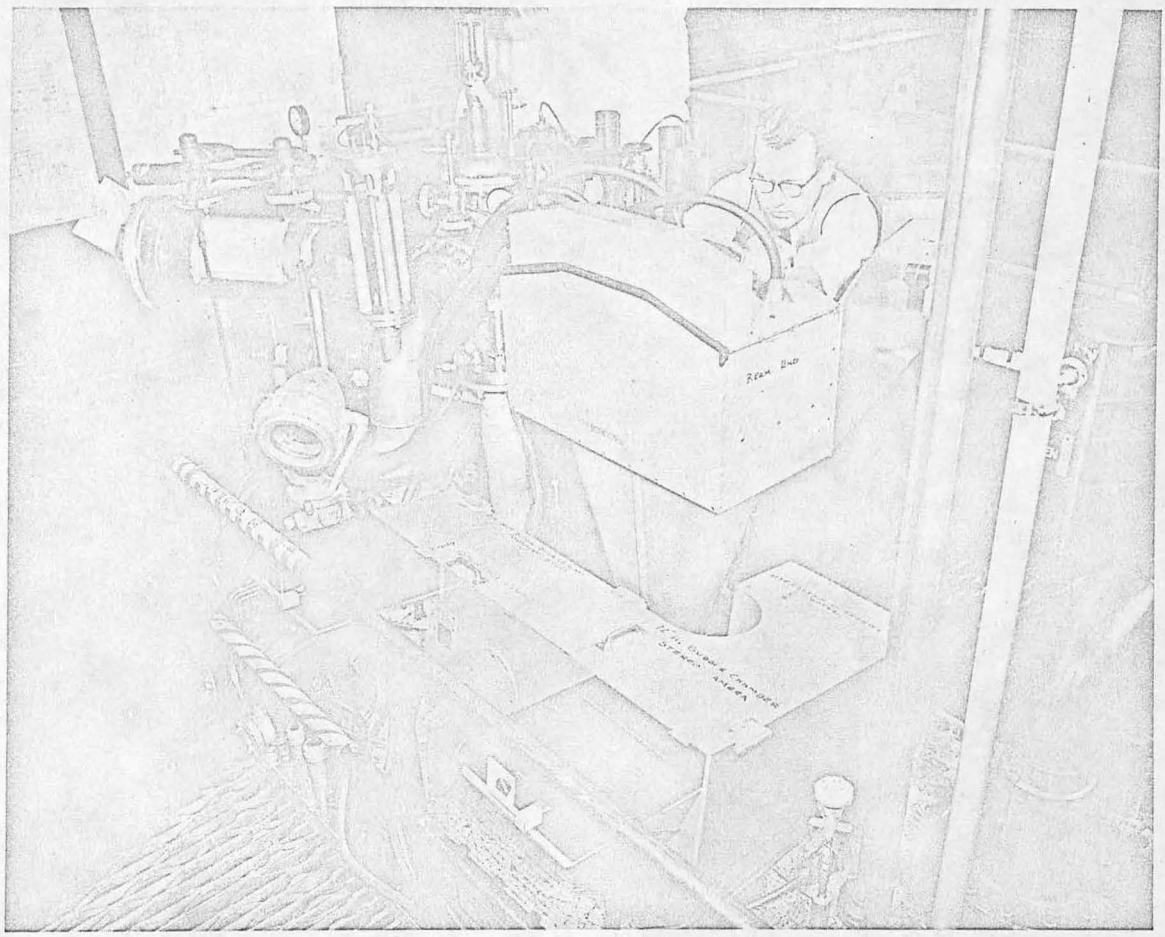

ZN-3302

Fig. 30. Tri-stereo camera for the Berkeley 72-inch bubble chamber.

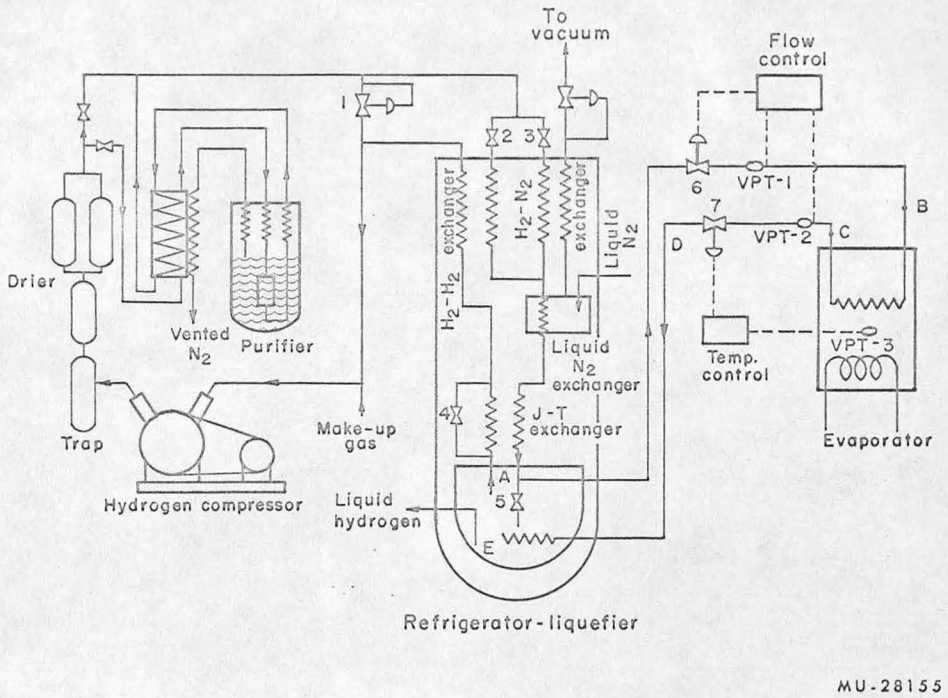

Fig. 31. Schematic flow diagram of hydrogen refrigeration system for the Berkeley 72-inch bubble chamber.

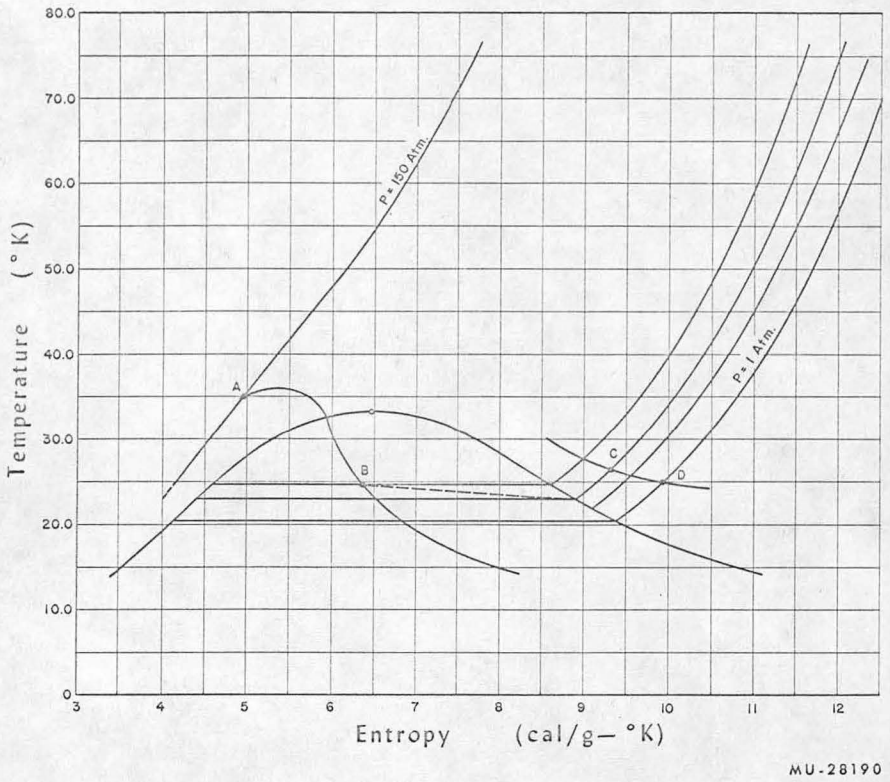

Fig. 32. Temperature - entropy diagram of hydrogen, showing control system operation of the hydrogen refrigerator for the Berkeley 72-inch bubble chamber.

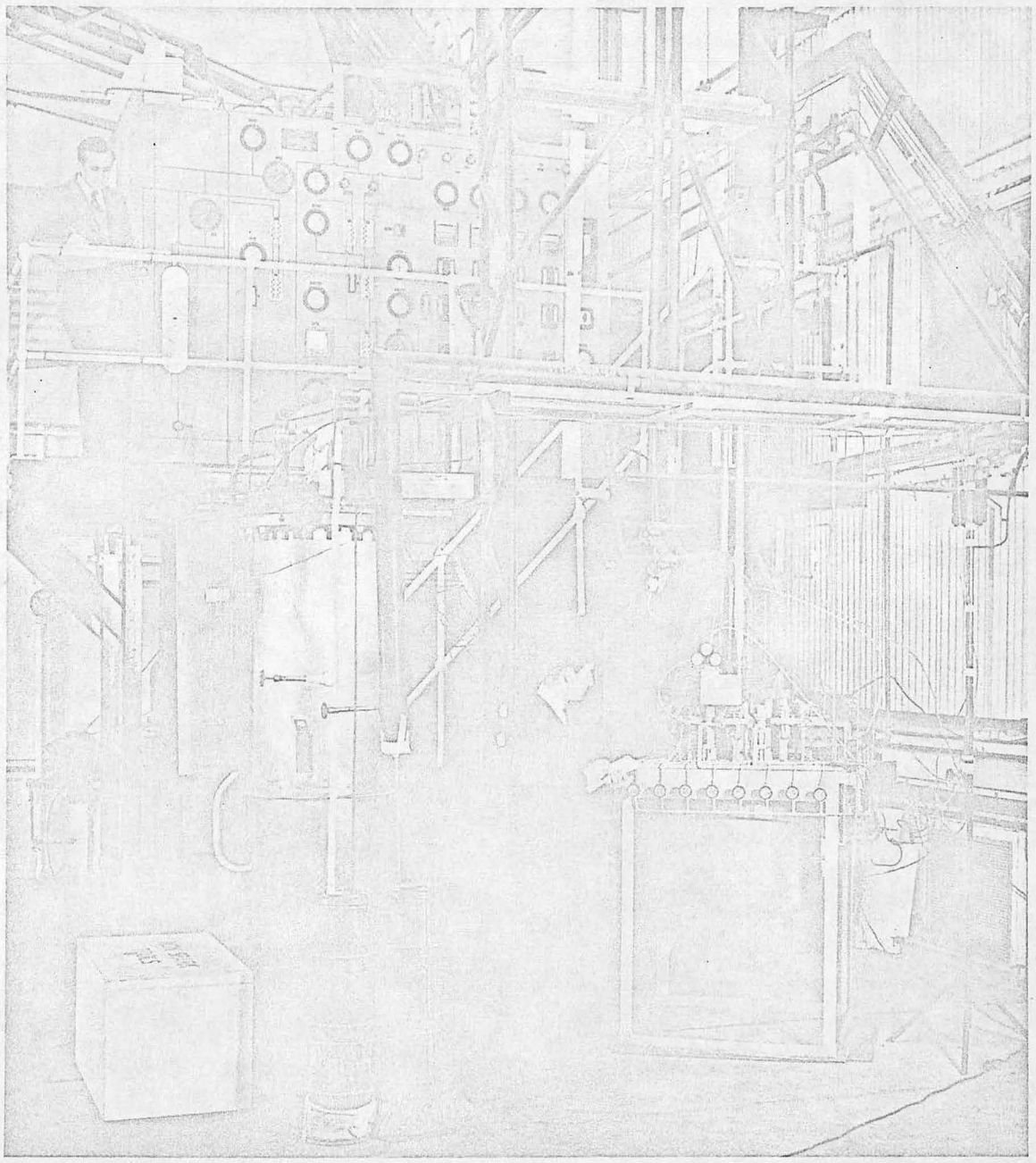

ZN-3305

Fig. 33. Refrigerator control board for the 60-inch British National bubble chamber. (Simulated refrigerator load, left foreground; control-valve assembly at right.)

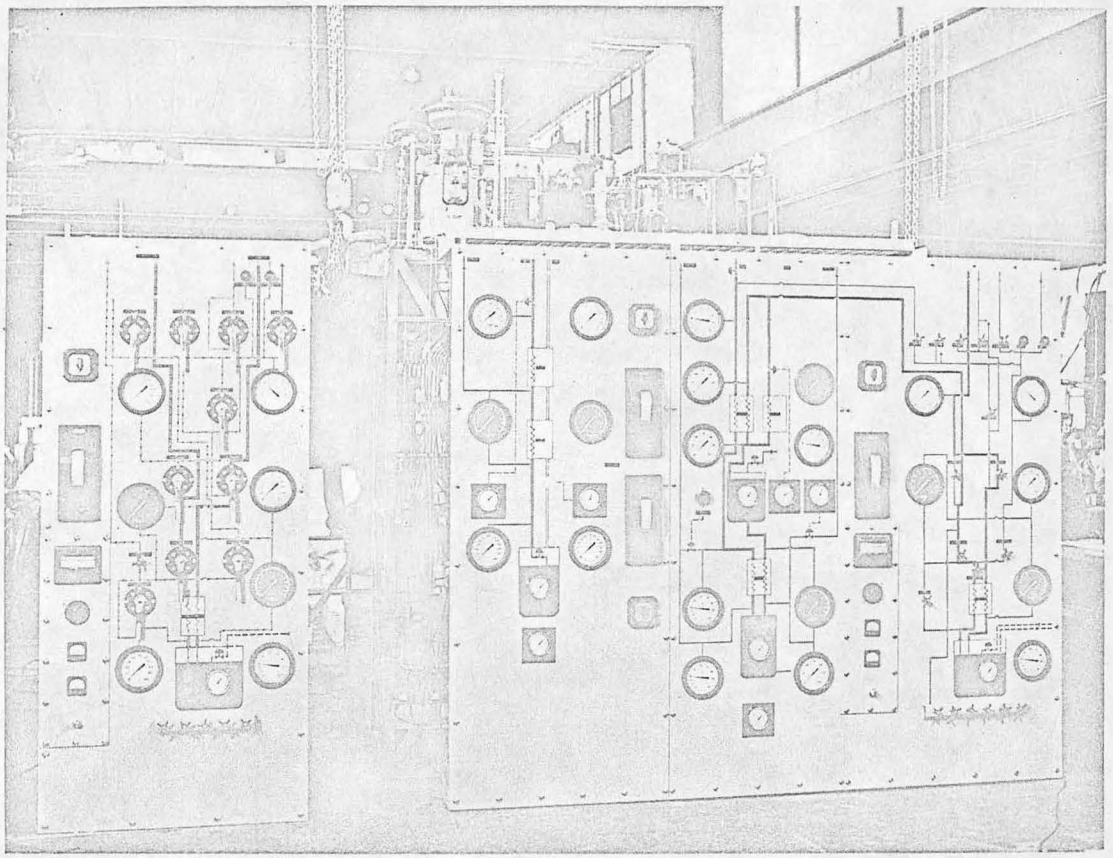

ZN-3306

Fig. 34. Hydrogen refrigeration system for the 80-inch Brookhaven bubble chamber. From left to right: low-pressure hydrogen purifier, nitrogen refrigerator-liquefier, hydrogen refrigerator, and high-pressure hydrogen purifier. (Courtesy Cryogenic Engineering Co.)

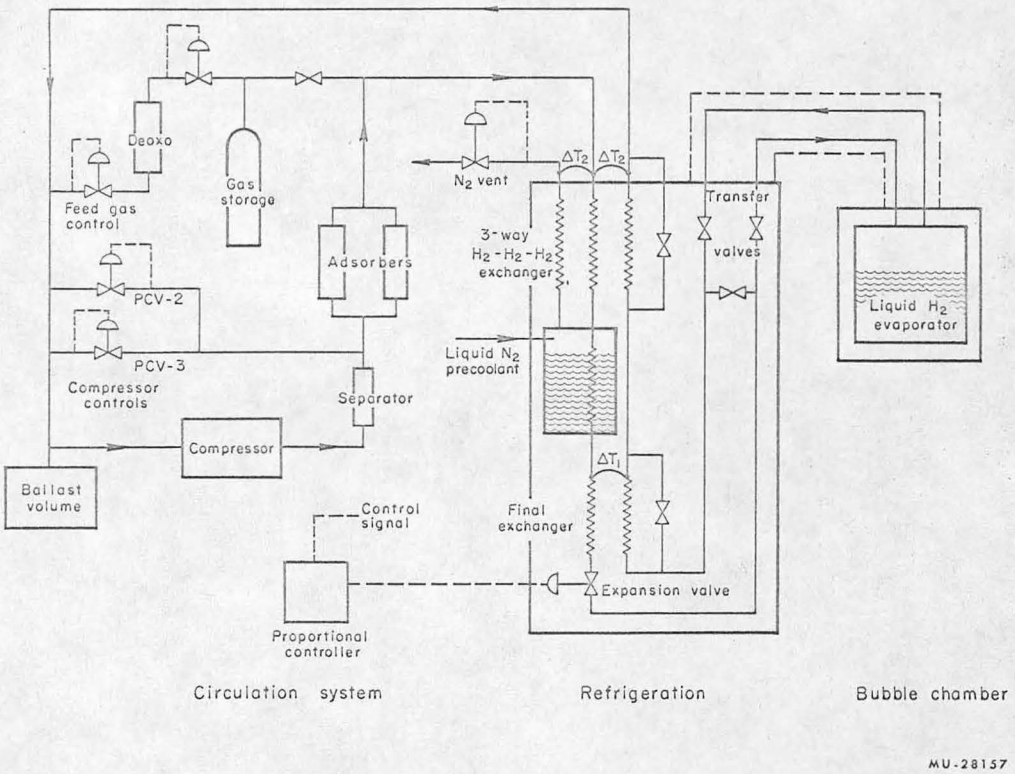

Fig. 35. Schematic arrangement of the hydrogen refrigeration system for the Berkeley 15-inch bubble chamber.

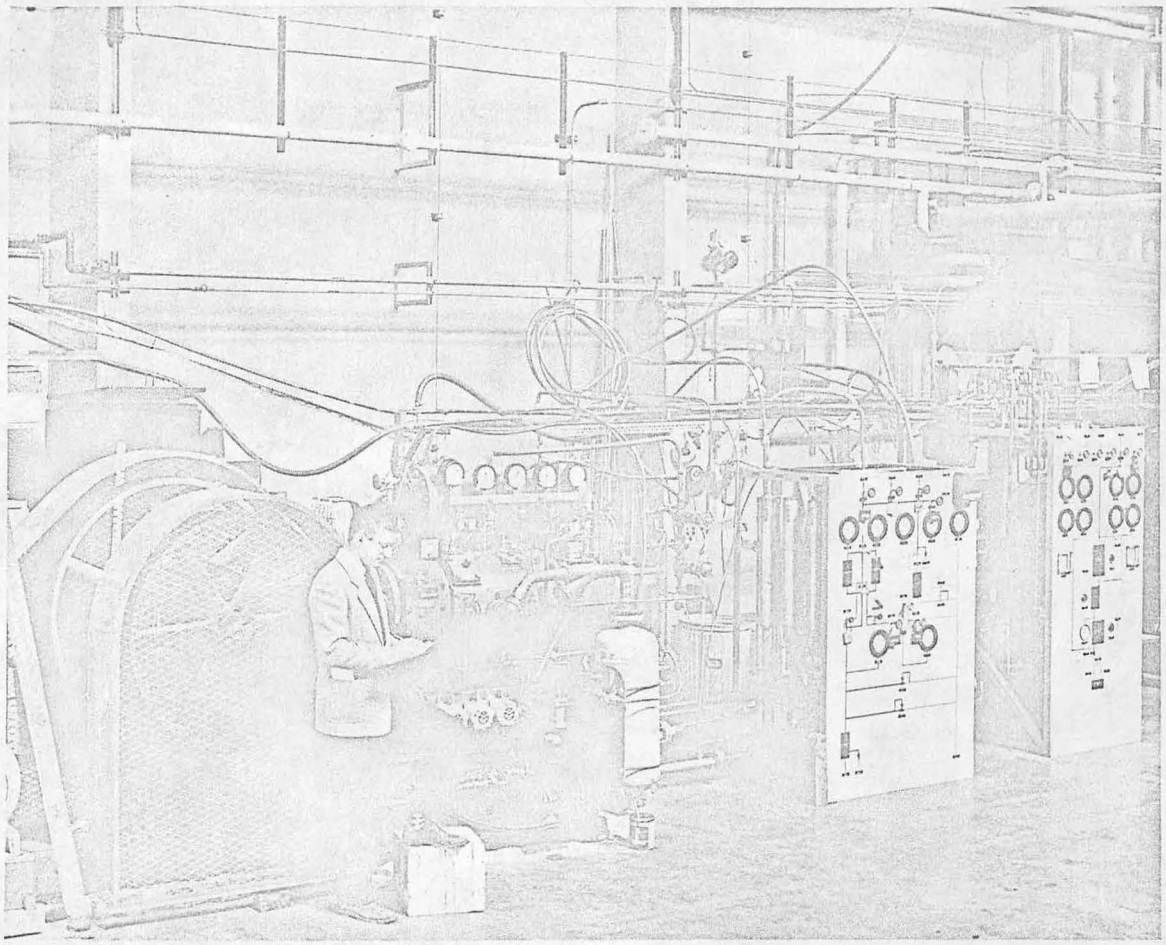

ZN-3303

Fig. 36. Refrigeration system for the Berkeley 15-inch bubble chamber.

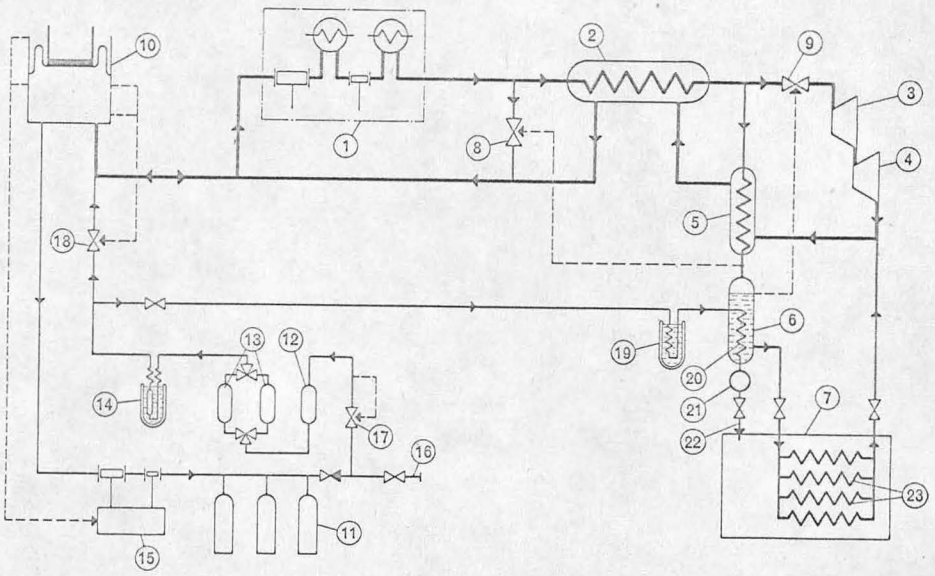

Fig. 37. Flow diagram of the CERN 2-meter hydrogen refrigeration plant.

1 Oilfree labyrinth-piston compressor
2 Main counterflow heat exchanger
3,4 Turbines
5 Condenser
6 Liquid reservoir
7 Bubble chamber
8 Bypass regulating valve
9 Throttle valve
10 Dry gasometer
11 Battery of high-pressure storage cylinders
12 Oxygen removal unit
13 Interchangeable gas driers
14 Low-temperature adsorber
15 Recovery compressor
16 Raw-gas inlet
17 Pressure regulating valve
18 Filling valve
19,20 Precoolers for chamber filling
21 Ultra-low-temperature adsorber
22 Filling line to chamber
23 Heat exchangers of chamber

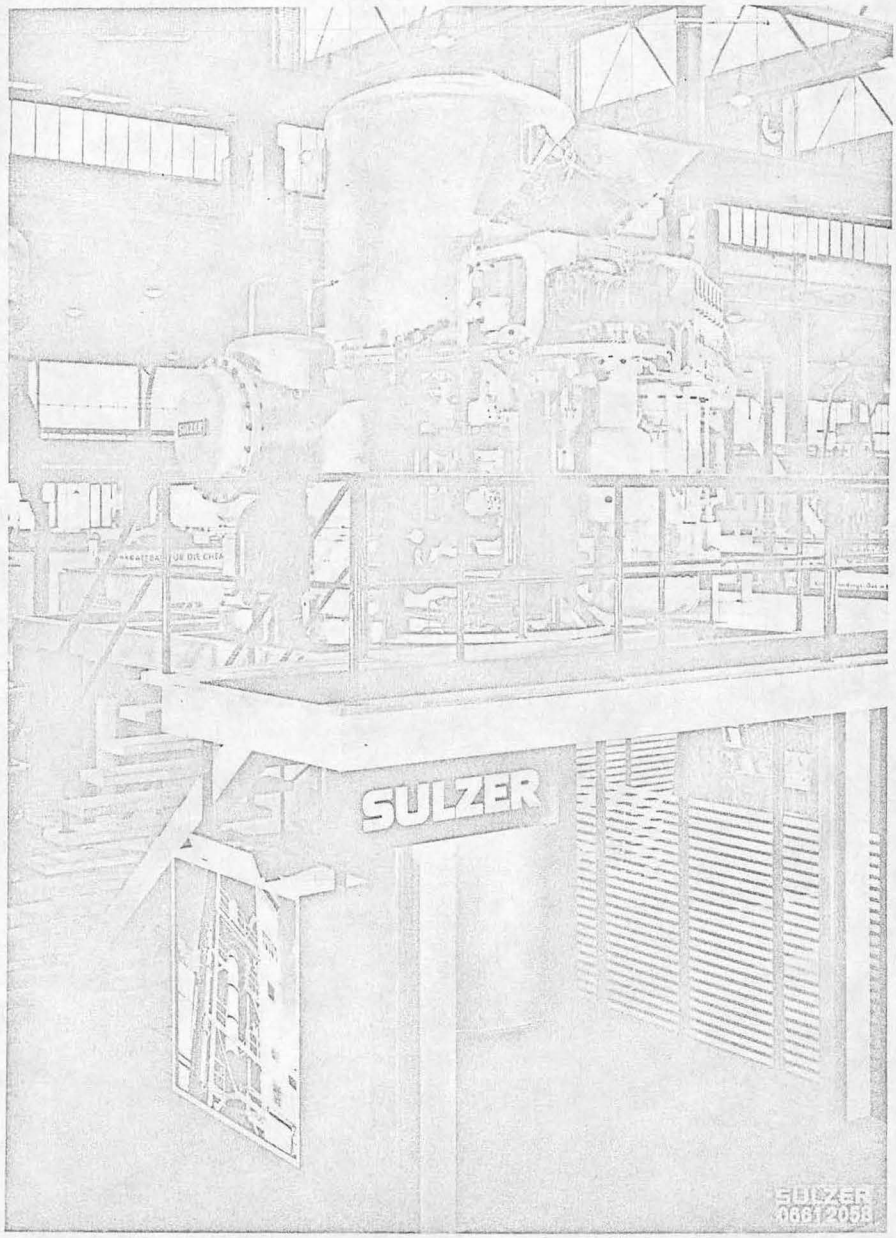

ZN-3307

Fig. 38. The CERN 2-meter hydrogen refrigerator.

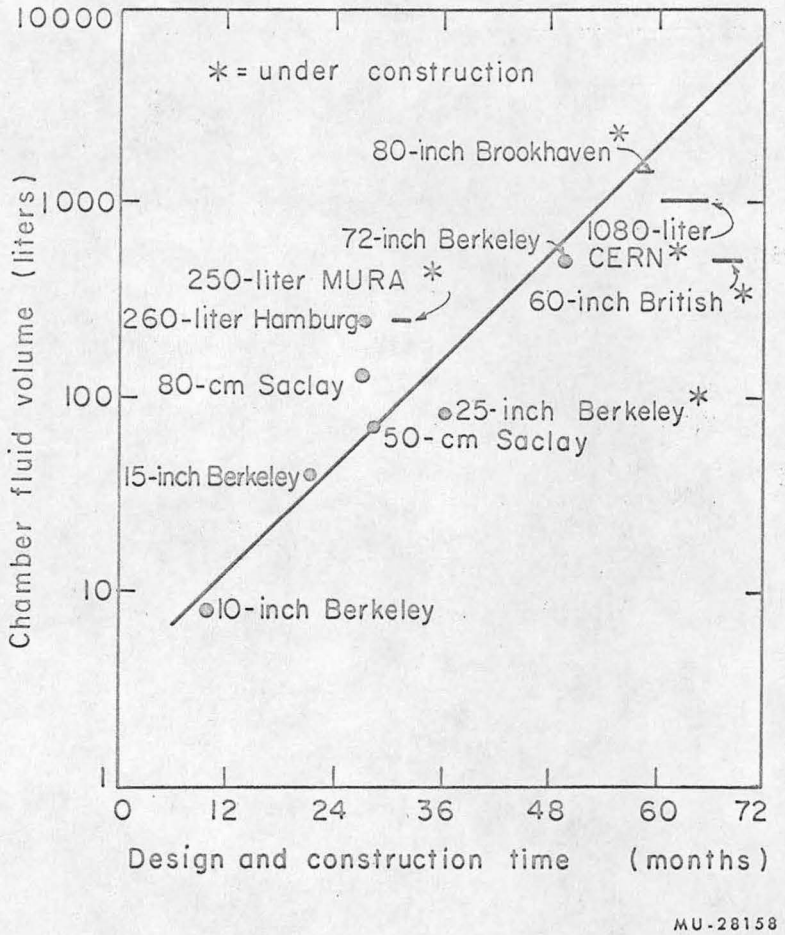

Fig. 39. Approximate total time required to build a bubble chamber (from conception to operation) as a function of chamber volume.

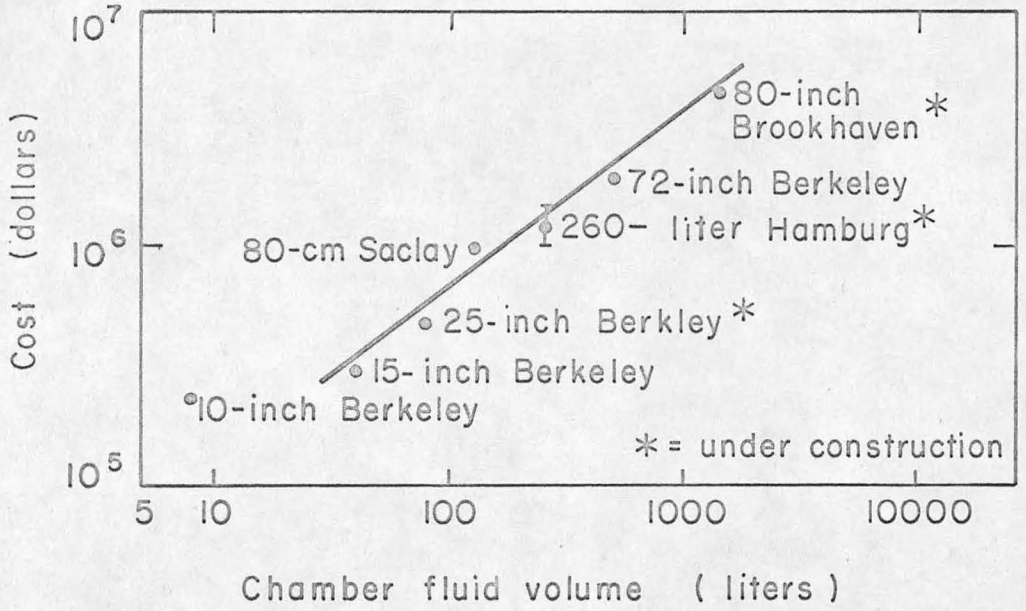

MU-28159

Fig. 40. Approximate cost to build a bubble chamber, as a function of chamber volume.

Table I. Chemical analysis of the 72-inch bubble chamber casting.

LRL specification		Analysis as cast	
		(1)	(2)
Ni	13-15	13.2	14.98
Cr	16-19	17.2	16.30
C	0.04-0.08	0.06	0.06
Mn	1.5 max	0.43	0.31
Si	1.5 max	0.38	0.48
S	0.04 max	0.023	0.02
P	0.04 max	0.024	0.03
Mo	0.04 max		0.10
N			0.04

Heat-treatment: 2000-2050°F water-quenched to room temperature

Yield strength (measured): 38 700 psi

Tensile strength (measured): 76 400 psi

Elongation percent (2 in.): 39%

Reduction in area: 41.7%

Electrical resistivity (measured by NBS):

T^0K	Resistivity, ohm-cm
300	80×10^{-6}
77	58×10^{-6}
20	55×10^{-6}

Table II. Chemical analysis of bubble chamber body stainless steels.

	72-inch Berkeley		80-inch Brookhaven		2-meter - CERN
Type	Modified CF-8		Kromarc-55		
Analysis	Range	Aim	Range	Aim	
Carbon	0.04 max	less	0.05 max	0.04	0.03
Manganese	1.5 max		9.00-1200	11	0.85-1.15
Silicon	1.5 max	less	0.50 max		0.30-0.50
Phosphorus	0.03 max		0.03 max		0.015 max
Sulphur	0.03 max		0.03 max		0.015 max
Chromium	16-19	18	15.00-18.00	16	17-18
Nickel	13-15	14.5	18.00-22.00	19	14.5-15.5
Molybdenum	0.5 max		1.75-2.75	2.25	
Nitrogen					0.04 max
At 20° C, minimum tensile yield point (0.2%) (psi)	32 000		25 000 to 28 000		
Ultimate (psi)	88 500		56 200		
At 20° K, minimum tensile yield point (psi)			89 000		
Ultimate (psi)			106 000		
Martensite start temp. (° F)	-620	-700[a] -1070	-2400	-1600	-760 -970
Martensite deformation temp. (° F)	-120	-200[a] - 580	-1900	-1100	-260 -470

[a] Actual

Table III. Breaking stress of BSC-2 optical glass. Median values from probability plots. A - abraded; U - unabraded.[a]

Condition	Rate stress increase lb/in.^{2}-sec	Breaking stress lb/in.^{2}			
		296°K	194°K	76°K	20°K
A	800	7 500	9 500	10 400	10 400
A	10	5 500	7 500	10 400	10 600[b]
A	1	5 000	6 400[b]	10 400[b]	10 200[b]
U	800	10 400		18 000	

[a]Reference 30.

[b]Fewer than 10 specimens.